AGU PUBLICATIONS

JGR

Journal of Geophysical Research: Biogeosciences

RESEARCH ARTICLE

10.1002/2015JG003190

Key Points:

- Climate change and forestry will have a limited impact on boreal [DOC]
- Climate and forestry effects are not additive at a local scale
- Climate and forestry effects are additive at a landscape scale

Correspondence to:
M. N. Futter,
martyn.futter@slu.se

Citation:
Oni, S. K., T. Tiwari, J. L. J. Ledesma, A. M. Ågren, C. Teutschbein, J. Schelker, H. Laudon, and M. N. Futter (2015), Local- and landscape-scale impacts of clear-cuts and climate change on surface water dissolved organic carbon in boreal forests, *J. Geophys. Res. Biogeosci.*, *120*, 2402–2426, doi:10.1002/2015JG003190.

Received 24 AUG 2015
Accepted 23 OCT 2015
Accepted article online 28 OCT 2015
Published online 25 NOV 2015

Local- and landscape-scale impacts of clear-cuts and climate change on surface water dissolved organic carbon in boreal forests

Stephen K. Oni[1], Tejshree Tiwari[1], José L. J. Ledesma[2], Anneli M. Ågren[1], Claudia Teutschbein[3], Jakob Schelker[4], Hjalmar Laudon[1], and Martyn N. Futter[2]

[1]Department of Forest Ecology and Management, Swedish University of Agricultural Sciences, Umeå, Sweden, [2]Department of Aquatic Science and Assessment, Swedish University of Agricultural Sciences, Uppsala, Sweden, [3]Department of Earth Sciences, Uppsala University, Uppsala, Sweden, [4]Department of Limnology and Bio-Oceanography, University of Vienna, Vienna, Austria

Abstract Forest harvesting and climate change may significantly increase concentrations and fluxes of dissolved organic carbon (DOC) in boreal surface waters. However, the likely magnitude of any effect will vary depending on the landscape-element type and spatial scale. We used a chain of hydrological, empirical, and process-based biogeochemical models coupled to an ensemble of downscaled Regional Climate Model experiments to develop scenario storylines for local- and landscape-scale effects of forest harvesting and climate change on surface water DOC concentrations and fluxes. Local-scale runoff, soil temperature, and DOC dynamics were simulated for a range of forest and wetland landscape-element types and at the larger landscape scale. The results indicated that climate change will likely lead to greater winter flows and earlier, smaller spring peaks. Both forest harvesting and climate change scenarios resulted in large increases in summer and autumn runoff and higher DOC fluxes. Forest harvesting effects were clearly apparent at local scales. While at the landscape scale, approximately 1 mg L^{-1} (or 10%) of the DOC in surface waters can be attributed to clear-cuts, both climate change and intensified forestry can each increase DOC concentrations by another 1 mg L^{-1} in the future, which is less than that seen in many waterbodies recovering from acidification. These effects of forestry and climate change on surface water DOC concentrations are additive at a landscape scale but not at the local scale, where a range of landscape-element specific responses were observed.

1. Introduction

The boreal forest, which covers much of the northern hemisphere landmass, plays a pivotal role in the global carbon cycle [*Apps et al.*, 1993; *Magnani et al.*, 2007]. Not only are the wood and other biomass products from boreal forests economically important but they are widely used for climate change mitigation through fossil fuel substitution. Boreal soils store up to 500 Gt of organic carbon (C) [*Pan et al.*, 2011], large amounts of which are exported as dissolved organic carbon (DOC) to surface waters [*Battin et al.*, 2009; *Tranvik et al.*, 2009], forming an important component of the global carbon budget [*Aufdenkampe et al.*, 2011; *Cole et al.*, 2007; *Öquist et al.*, 2014]. DOC is a substrate for microbial respiration and contributes to CO_2 evasion to the atmosphere [*Koehler et al.*, 2014; *Wallin et al.*, 2013] or can be a pathway for C accumulation in lake or river sediments [*Cole et al.*, 2007]. However, with the changing climate and increasing pressure of forestry, there are additional stresses on boreal stream DOC, which may have severe consequences.

Much of the boreal forest is in a delicate balance between acting as a C source or sink [*Laudon et al.*, 2013b; *Tetzlaff et al.*, 2013]. Climate change will likely affect net primary production and increase litter production by altering the length of the growing season and climatic conditions [*Jansson et al.*, 2008; *Kleja et al.*, 2008]. It also affects soil organic matter mineralization rates as soils become warmer and wetter [*Davidson and Janssens*, 2006]. Modeling studies suggest both large increases [*Larsen et al.*, 2011] and small changes [*Holmberg et al.*, 2014] in boreal lake DOC concentrations ([DOC]) under a changing climate. However, it has also been shown that the magnitude of simulated change in [DOC] under a changing climate depends on the modeling approach [*Oni et al.*, 2014].

Similarly, forest harvesting can have significant impacts on water quality [*Kreutzweiser et al.*, 2008; *Laudon et al.*, 2011b]. The mechanisms causing increases in [DOC] are related primarily to reductions in interception

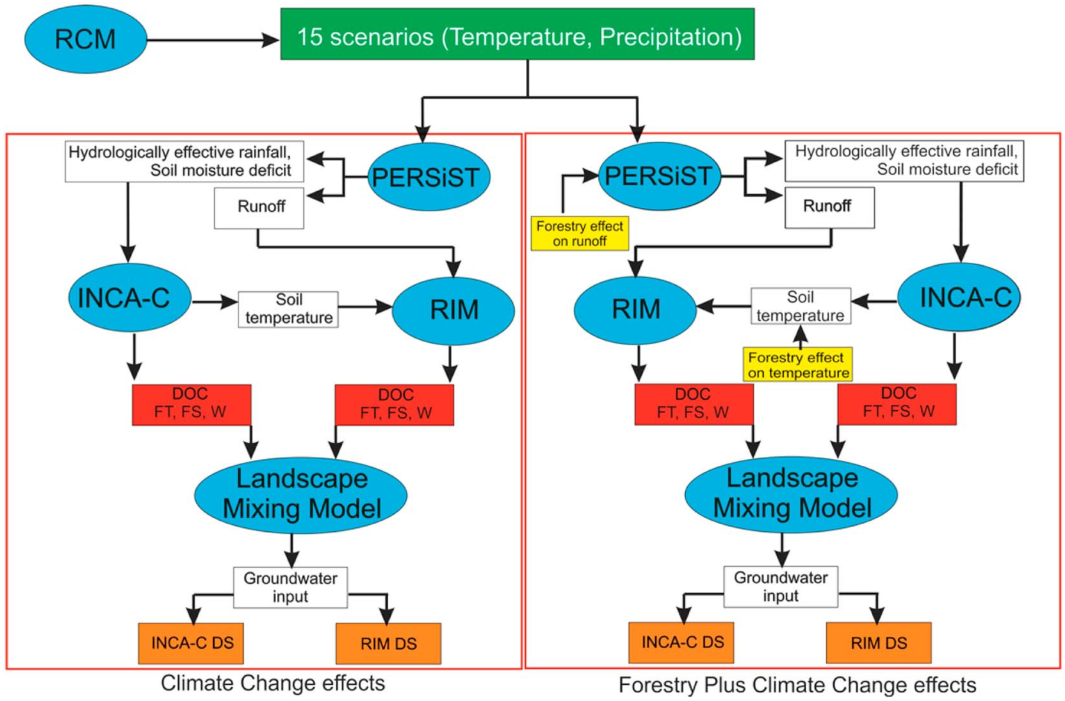

Figure 1. Conceptual diagram showing connections in the chain of models used in assessing present and future local- and landscape-scale climate and forestry effects on stream DOC concentration and fluxes. Measured climate data and downscaled outputs from 15 Regional Climate Model (RCM) experiments feed into the hydrological model (PERSiST). Outputs from the PERSiST model are used as hydrological forcings to the local-scale biogeochemical models (INCA-C and RIM) for the different landscape end-members (FT = Forest on till, FS = Forest on sediment, W = Wetland, DS = downstream). The output of the local-scale biogeochemical models feed into the large-scale landscape mixing model (LMM), where they are combined with a DOC signal from deep groundwater flow paths (as a function of discharge).

and evapotranspiration. Forest harvesting can lead to increased winter snow accumulation and spring melts [*Schelker et al.*, 2013b] and higher runoff compared to intact forests [*Futter et al.*, 2010]. Warmer soils may also be observed following clear-cuts as the shading effect of tree cover is absent [*Schelker et al.*, 2013a]. There are well-documented studies showing increases in DOC concentrations and fluxes following clear-cutting in the boreal forest [*Palviainen et al.*, 2014; *Schelker et al.*, 2012]. Studies of forestry impacts on surface water DOC are typically based on paired catchments [*Palviainen et al.*, 2014; *Schelker et al.*, 2012] or long-term monitoring [*Lepistö et al.*, 2014]. There have been some attempts to upscale local results to a regional level. For example, *Schelker et al.* [2014] showed that when forest harvesting affects more than a critical threshold of catchment area, detectable increases in downstream [DOC] will occur. However, to date, there have been no studies on the potential combined effects of future forest management and climate change on surface water [DOC] and its implications for the overall C balance in boreal forests.

Currently, less than 1% of productive Swedish forests are harvested annually [*Christiansen*, 2014], but this may increase in the future, both due to greater demand and faster forest growth. Industrialized forestry is expected to grow in many countries due to increasing demands for forest products for bioenergy to meet green energy targets including the EU Renewable Energy Directive [*Egnell et al.*, 2011]. In recent years, Sweden has pursued more intensive forest harvesting as a way of fulfilling the requirements of the EU renewable energy directive [*Egnell et al.*, 2011]. A major concern is how intensified forest activities will impact water quality and particularly DOC.

The boreal forest can be conceptualized as a mosaic of landscape-element types defined by vegetation cover, drainage, and Quaternary geology. These landscape element types display markedly different biogeochemical and hydrological signatures. In the boreal regions of Sweden, landscape-element types representing forest on till, forest on sediment, and wetlands define the mosaic. Forests on till are typically found above the highest coastline, while forests on lacustrine or marine sediments are found below the highest coastline.

Wetlands, usually mires, are found in areas of impeded drainage. Each of these landscape-element types has a distinct biogeochemical signature [*Grabs et al.*, 2012; *Ledesma et al.*, 2013]. At a larger landscape scale, much of the unique signature can be lost [*Ågren et al.*, 2014] and local-scale effects of forest harvesting on water quality diluted [*Schelker et al.*, 2014]. While climate change and forestry will affect all landscape element types, much remains unknown about the individual local-scale responses, or their combined effect at a downstream landscape scale.

Spatial scale is extremely important when assessing the impacts of anthropogenic activity on water quality. Forestry impacts on water quality are most apparent at small spatial scales typical of individual stands or headwaters [*Cui et al.*, 2012; *Futter et al.*, 2010; *Palviainen et al.*, 2014; *Sanders and McBroom*, 2013] and can be masked or impossible to detect at the river mouths of large catchments [*Lepistö et al.*, 2014]. In what follows, we refer to two spatial scales: the local and the landscape. The former has a spatial extent of approximately 10 ha and includes individual forest stands and headwater catchments. The latter has a spatial extent of tens of square kilometers and larger and is representative of medium size rivers and mesoscale catchments. Landscape-scale water quality is not simply the sum of local-scale inputs but can also include the effects of in-stream processing or inputs from deep groundwaters [*Hagedorn et al.*, 2000; *Tiwari et al.*, 2014].

Both empirical [*Hejzlar et al.*, 2003; *Larsen et al.*, 2011] and process-based [*Futter et al.*, 2009; *Holmberg et al.*, 2014] models have been used to project future [DOC]. There are advantages and disadvantages to each approach; empirical models generally produce better goodness of fit statistics [*Futter and de Wit*, 2008] but process-based modes are considered to be more appropriate for simulating conditions outside the range of current observations [*Leavesley*, 1994; *Adams et al.*, 2012; *Crossman et al.*, 2014]. Models can be used to simulate hydrological and biogeochemical processes at different scales, ranging from hillslopes to landscapes (Figure 1) [*Futter et al.*, 2007; *Seibert et al.*, 2009; *Winterdahl et al.*, 2011]. By using an ensemble of biogeochemical models and climate scenarios, it is possible to ensure that the range of outcomes reflects different spatial scales as well as the different biogeochemical processes operating within the catchment. This range of possible outcomes contributes to the development of storylines about possible futures. While storylines can be based on quantitative outputs, they are more useful as internally consistent plausible, qualitative descriptions of what may happen, not necessarily what will happen [*Börjeson et al.*, 2006; *Milestad et al.*, 2014; *Rounsevell and Metzger*, 2010].

Here we present simulations based on an ensemble of hydro-biogeochemical models and downscaled climate models outputs (Figure 1) to develop storylines about possible forest harvesting and climate change effects on local- and landscape-scale seasonal and interannual patterns in DOC concentrations and fluxes in boreal streams. We used the steady state empirical Riparian Flow-Concentration Integration Model (RIM) [*Seibert et al.*, 2009] and the dynamic, process-based Integrated Catchment Model for Carbon (INCA-C) [*Futter et al.*, 2007] to reflect different scales of processes occurring in the boreal landscape (Figure 1). These two modeling approaches have been used previously to simulate DOC dynamics in headwater boreal catchments representative of the landscape element types simulated here [*Futter et al.*, 2009, 2011; *Futter and de Wit*, 2008; *Oni et al.*, 2014; *Winterdahl et al.*, 2011, 2014]. However, other models, such as those developed by *Naden et al.* [2010] or *Temnerud et al.* [2014], could also have been used. A landscape mixing model is used to integrate signals from headwater to downstream. Local-scale inputs do not necessarily completely define landscape-scale water quality signatures mainly because, as transit times increase, the influence of groundwater discharge becomes more prominent [*Ågren et al.*, 2014] and there is more opportunity for aquatic processing of carbon [*Müller et al.*, 2013]. Thus, the effect of groundwater at the landscape scale was also included (Figure 1).

We addressed the following questions related to the development of plausible, internally consistent storylines about future water quality in the boreal forest: (i) Do empirical and process-based models of surface water DOC give similar projections of future surface water quality under climate change and more intensive forest harvesting? (ii) Are the projected effects of clear-cutting on surface water quality the same for different landscape-element types? (iii) What are the interactions between climate change and forestry effects on surface water DOC concentrations and fluxes at local and landscape-scales?

2. Materials and Methods

The climate and forestry scenarios presented here are summarized in Table 1. All results were based on measurements made at the Krycklan catchment and Balsjö experimental clear-cut (Figure 2). All present-day

Table 1. Summary of the Scenarios, Their Data Sources, and Properties

Period	Climate Forcing	Abbreviation	Name	Scale	Brief Description of Key Features
Present	Observed (Krycklan) meteorology.	KC	Krycklan calibrated	Local, Landscape	Calibrated to streamflow (C7) and [DOC] (C2, C4, and C20) from Krycklan study catchments
		PDF	Present-Day Forestry	Local	KC parameterization adjusted to reproduce runoff and soil temperature effects of clear-cutting observed at Balsjö
		BAU	Business as Usual	Landscape	KC and PDF were provided as inputs to the Landscape Mixing Model (LMM) using current climate with an assumption of 0.86% of the area felled annually
		IFH	Intensive forest harvest	Landscape	KC and PDF were provided as inputs to the LMM using current climate and an assumption of 1.72% of the area felled annually
Future	Ensemble of 15 downscaled RCM experiments	CC	Climate Change	Local, Landscape	Based on KC hydrological and biogeochemical model parameterization with future climate from RCMs
		FF	Future Forestry	Local	Based on PDF hydrological and biogeochemical model parameterization with future climate from RCMs
		CCF	Climate Change and "Business as Usual" Forest Harvest	Landscape	CC and FF were provided as inputs to the LMM using future climate with an assumption of 0.86% of the area felled annually
		CCI	Climate change and intensive forest harvesting	Landscape	CC and FF were provided as inputs to the LMM using future climate with an assumption of 1.72% of the area felled annually

simulations were forced by observed meteorological data from the Krycklan catchment study. Future projections were based on model parameter sets obtained during present-day simulations and forced by outputs from an ensemble of downscaled outputs from 15 RCM experiments.

2.1. Krycklan Catchment Study

The modeling and analyses presented here were performed using data from the Krycklan catchment (68 km^2) (Figure 2), a well-instrumented and monitored site representative of the boreal landscape [*Laudon et al.*, 2013a]. The catchment is located in northern Sweden (64°16′N, 19°46′E) and has been set aside for process-based, experimental, and hypothesis-driven research needed to improve scientific knowledge, policy, and management of boreal ecosystems. Across the whole Krycklan catchment, Quaternary till deposits with low permeability cover the upper part (51%) of the catchment while thick freely draining marine-derived glacio-fluvial sediments cover the lower parts (49%) with deep characteristic incised channeled streams [*Ågren et al.*, 2007]. Forest soils are mostly well-developed iron podzols with organic carbon-rich riparian zones. Catchment elevation ranges from 126 to 372 m above sea level, and the highest postglacial coastline crosses the catchment at around 255–260 m [*Ågren et al.*, 2007]. In areas with low slopes, water tends to accumulate to form minerogenic mires, characterized by acidophilic *Sphagnum* species. Forests (87%), wetlands (peaty mires; 9%), arable land (3%), and lakes (1%) cover the catchment, and low-intensity forestry is conducted throughout. The dominant tree species in the catchment are Norway spruce (*Picea abies*, 27%) and Scot pine (*Pinus sylvestris*, 63%). The remaining 10% are deciduous trees, mainly birches (*Betula spp.*) that are found on and around riparian zones.

The catchment has a long-term (1981–2012) mean annual temperature of 1.8°C (peaking in July), mean annual precipitation of 631 mm yr^{-1} (±102 mm yr^{-1}), and mean annual runoff of 324 mm yr^{-1} (± 96 mm yr^{-1}). Up to 50% of annual precipitation falls as snow in the winter, and the snowpack can last up to 170 days (November–May) [*Laudon et al.*, 2013a; *Oni et al.*, 2013]. Subsurface pathways dominate the delivery of runoff to streams and rivers. This influences the overall hydrology of Krycklan between limited groundwater influences at the headwaters to a dominating groundwater contribution at the outlet of the 68 km^2 catchment. Long-term hydrologic simulations were based on daily precipitation and air temperature monitored at a weather station at the center of the Krycklan catchment and specific discharge data from site C7 (Figure 2) [*Laudon et al.*, 2013a]. Site C7 has been used because it has the longest consistent record of streamflow of any of the catchments in Krycklan.

At the Krycklan catchment outlet, water chemistry can be conceptualized as a time-dependent mixture of local-scale upstream surface waters and landscape-scale groundwater contributions, in which the dominant

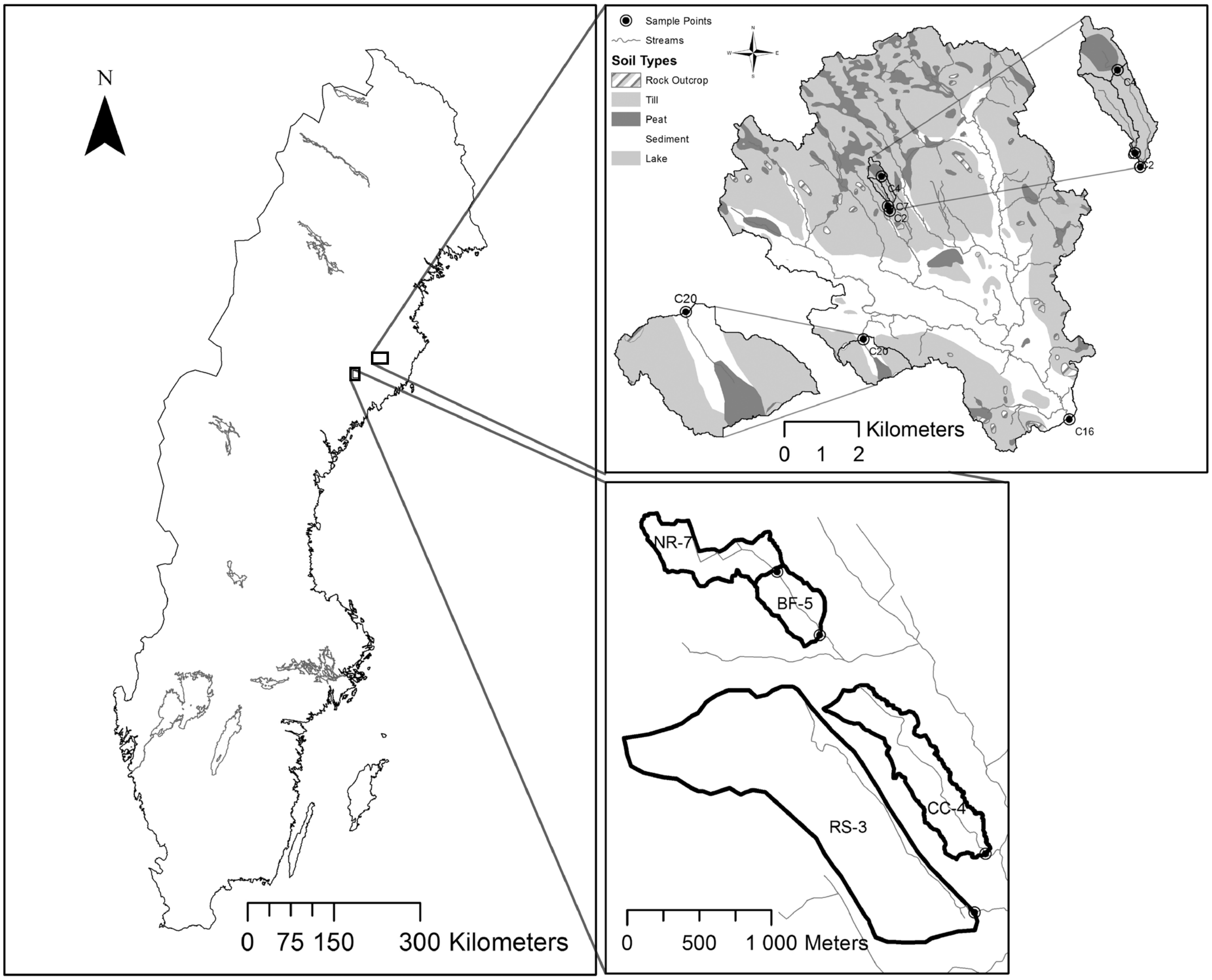

Figure 2. Map showing the location of the study catchments within (a) Sweden, (b) the Krycklan catchment, and (c) the Balsjö clear-cut experiment. The Krycklan map (Figure 2b) shows the location of the forest on till (C2), wetland (C4), and forest on sediment (C20) headwater catchments used in the local-scale simulations presented here. The landscape-scale simulations were made for the catchment outlet (C16). Balsjö data used here were from the clear-cut (CC4, BF5) and reference (NR-7) subcatchments.

landscape types (forest on till, forest on sediment, and wetlands) exhibit unique biogeochemical signatures. While forests on till and wetlands are DOC rich, forests on sediments are characterized by lower [DOC] [*Ågren et al.*, 2014]. Three well-monitored headwater catchments representative of forests on till (C2), wetlands (C4), and forests on sediments (C20) were used to characterize local-scale DOC dynamics (Figure 2) [*Laudon et al.*, 2011a, 2013a; *Oni et al.*, 2013].

2.2. Balsjö Paired Catchment Clear-Cut Experiment

Simulations of forest harvesting effects on hydrology and soil conditions influencing DOC production and export were based on observations made between 2005 and 2011 for hydrology and 2009 for soil temperature from the Balsjö paired catchment study (64°2′N, 18°56′E; 22.9 km^2). Balsjö is close to Krycklan, about 70 km west of the Baltic coast in northern Sweden (Figure 2). Studies at Balsjö have documented the effects of clear-cutting on soil temperature [*Schelker et al.*, 2013a], hydrologic flow paths [*Schelker et al.*, 2013b; *Sørensen et al.*, 2009b], and stream chemistry [*Laudon et al.*, 2009; *Löfgren et al.*, 2009; *Schelker et al.*, 2012; *Schelker et al.*, 2014; *Sørensen et al.*, 2009a]. The study includes an unharvested control catchment and two catchments with differing degrees of clear-cutting. The simulations used here were based on observations made at the unharvested NR7 reference catchment and the clear-cut catchments (Figure 2).

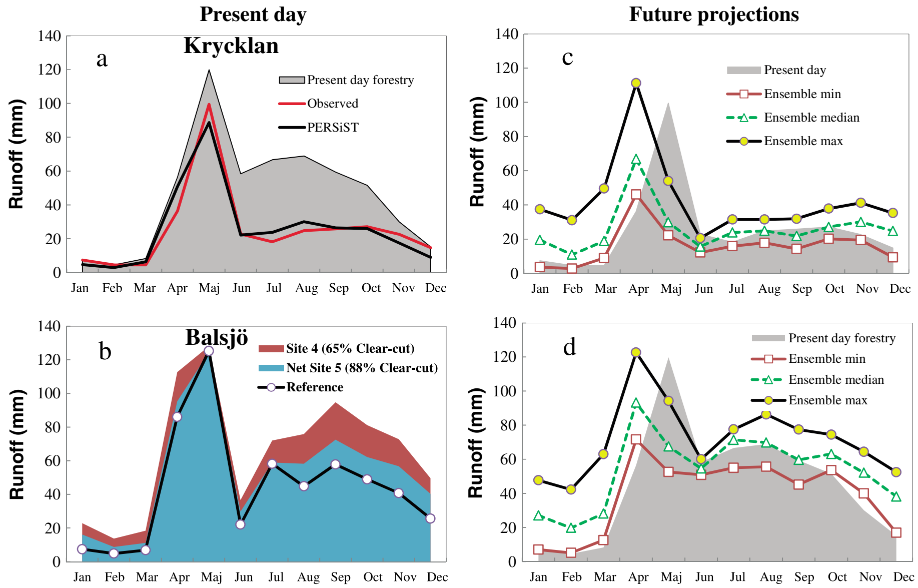

Figure 3. Monthly runoff summaries including present-day (a and b) and future (c and d) values. (a) Monthly average observed runoff, PERSiST model calibration for the KC scenario and the PDF scenario, which simulates clear-cut effects at Krycklan site C7 between 2005 and 2012. (b) Monthly average observed runoff at Balsjö clear-cut and control sites. The difference in runoff between control and clear-cut sites was used to identify parameter values for the PDF scenario. (c) A summary of results from the CC scenario with possible climate effects on runoff including the monthly minimum, maximum, and overall average runoff obtained from the ensemble of 15 RCMs. Average monthly present-day runoff from the KC scenario is included to facilitate comparison. (d) Results from the FF scenario which simulates possible local-scale combined effects of future climate change and forest harvesting on runoff dynamics. Average values from the PDF scenario are presented to facilitate comparison. Values in Figure 3d were obtained using the 15 RCM realizations and the PDF parameter set used for simulating present-day forestry.

Balsjö shares some similar attributes to Krycklan. Soils in Balsjö are dominated by well-drained till in recharge areas and mire-dominated discharge areas cover 15% of the catchment[*Schelker et al.*, 2013b]. Tree cover is also similar. The Balsjö catchment has annual temperature and precipitation of 0.6°C and 613 mm yr^{-1}, respectively, and a stable snow cover between November and May. Spring melt runoff occurred over an extended time period (April–May) at the Balsjö reference site (no clear-cut) but peaked later in May in Krycklan (Figure 3). The spring peak at Balsjö was higher than that in Krycklan (Figure 3), and both summer and autumn runoff were higher at the Balsjö reference site compared to Krycklan. No difference in spring melt runoff between the nonharvested reference site and the clear-cut sites in Balsjö (Figure 3) was observed. Forest clear-cuts at Balsjö have intensified the rate of snow accumulation and melt [*Schelker et al.*, 2013b], increased summer runoff [*Sørensen et al.*, 2009a], and increased summer soil temperatures [*Schelker et al.*, 2013a].

2.3. Climate Projections

Current (1981–2010) and future (2061–2090) simulations of precipitation and temperature were obtained from the ENSEMBLES project data archive [*Van der Linden and Mitchell*, 2009]. An ensemble of 15 regional climate models (RCMs) driven by different global climate models (GCMs) were used in the simulations presented here. The ensemble is further described in *Oni et al.* [2014]. Hereafter, individual members of the ensemble are referred to as RCM experiments. Each RCM experiment had a resolution of 25 km × 25 km and was run under the Special Report on Emissions Scenarios A1B. The A1B scenario is a medium-high emission-scenario based on a future assumption of strong economic growth and balance use of all sources of energy with an associated increase in the rate of greenhouse gas emissions [*Intergovernmental Panel on Climate Change*, 2007]. It is broadly comparable to Representative Concentration Pathway (RCP) 6.0/Shared Socio-Economic Pathway 2 (SSP2) in the new Representative Concentration Pathways (RCP) and Shared Socio-Economic Pathways (SSP) scenarios [*van Vuuren and Carter*, 2014]. Precipitation and temperature values were obtained by averaging the values of the RCM grid cell with center coordinates closest to the center of the catchment and of its eight neighboring grid cells. The spatial mismatch between RCM grid cell size (~625 km^2) and the size of the relatively small study catchments can, in combination with the often debated issue of systematic errors (so-called biases) in RCMs, heavily influence subsequent hydrological modeling results [*Ehret et al.*, 2012; *Muerth et al.*, 2013; *Teutschbein and Seibert*, 2012]. Postprocessing of the RCM data (i.e., bias correction) is therefore required. To bias-correct the RCM-simulated precipitation and temperature series, a distribution mapping procedure was used [*Déqué et al.*, 2007; *Ines and Hansen*, 2006], which has been used previously for climate change impact studies in Sweden [*Teutschbein and Seibert*, 2012, 2013]. The distribution mapping adjusts a theoretical cumulative distribution function (CDF) of RCM-simulated climate values so that it matches the observed CDF of observed temperature or precipitation (measured at a weather station within the Krycklan catchment). The Gamma distribution was used to simulate the CDF of precipitation events [*Piani et al.*, 2010], and a Gaussian distribution was used to bias correct temperature time series [*Teutschbein and Seibert*, 2012]. A precipitation threshold was introduced for each RCM so as to avoid distorting the precipitation distribution during dry conditions. This was needed as RCM outputs often include large numbers of days with light rains instead of dry conditions. Biases are assumed to be stationary, and the same correction algorithm (i.e., CDF parameters) was applied to both current and future climate conditions.

2.4. Forest Harvest Scenarios

Two forest harvest scenarios were used here: business as usual (BAU) representing current conditions and intensive forest harvesting (IFH) representing a plausible increase in harvest rate. According to the Swedish Statistical Yearbook of Forestry [*Christiansen*, 2014] 0.86% of productive forest land is clear-cut annually. Thus, the landscape-scale BAU clear-cut rate was set to 0.86% yr^{-1}. It should be noted that this value is slightly higher than the actual clear-cut rate at Krycklan, where approximately 25% of the catchment is not harvested. The IFH scenario assumed that forest harvesting will intensify due to shorter rotation periods and increasing demand for forest products for bioenergy. A doubling of clear-cut rates to 1.72% yr^{-1} was assumed to represent the maximum feasible increase in harvest intensity rates for the IFH scenario.

2.5. Biogeochemical Modeling

The biogeochemical modeling was performed as follows. Present-day (2005–2012) conditions were simulated in the following four steps: (i) A rainfall-runoff model: the Precipitation Evapotranspiration and Runoff Simulator for Solute Transport (PERSiST) [*Futter et al.*, 2014], was calibrated to long-term present-day (1981–2012) conditions. (ii) Outputs from the rainfall-runoff model (including soil moisture status) were then used as inputs to a series of local-scale landscape-element specific simulations (2005–2012) using INCA-C, a process-based model of DOC production and transport [*Futter et al.*, 2007, 2009]. (iii) Simulated flows from (i) and soil temperatures from (ii) were used as inputs to local-scale landscape-element specific simulations (2005–2012) using RIM, an empirical model for riparian and stream DOC dynamics [*Seibert et al.*, 2009]. Finally, (iv) landscape-scale DOC fluxes were estimated using local-scale, landscape-element-specific results from both models (ii) and (iii) as inputs to a landscape mixing model [*Cooper et al.*, 2000; *Tiwari et al.*, 2014] (Figure 1).

2.5.1. Hydrologic Modeling

The Precipitation, Evapotranspiration and Runoff Simulator for Solute Transport (PERSiST) is a catchment-scale, daily time scale rainfall-runoff model requiring inputs of precipitation and air temperature [*Futter et al.*, 2014]. Precipitation is partitioned into rain or snow depending on whether air temperature is above or below a user-specified threshold value. Canopy interception for snowfall and rainfall is simulated, and the model uses simple degree-day evapotranspiration and temperature-index snowmelt routines [*Futter et al.*, 2014]. PERSiST simulates the hydrologically effective rainfall (HER) and soil moisture deficit (SMD) time series needed for INCA-C (Figure 1). HER represents the fraction of precipitation that contributes to the runoff generation. SMD is the difference between maximum soil water holding capacity and an average soil water depth.

PERSiST was set up using four vertically stacked buckets through which precipitation was routed. The uppermost bucket was used to manage canopy interception as well as rain and snowmelt inputs, while the lower three buckets contributed to streamflow. These three buckets were representative of direct runoff having limited contact with the soil, soilwater, and shallow groundwater, respectively. All evapotranspiration was simulated in the soilwater bucket. The catchment was simulated as a single reach with one land cover type.

The model was calibrated using long-term (1981–2012) observed streamflow data from site C7 and meteorological data from the Krycklan weather station to simulate present-day (KC scenario) runoff conditions.

Manual calibration was first performed by fine tuning the parameters to minimize difference between the simulated and observed runoff. Model performance was assessed using Nash and Sutcliffe efficiencies (NSE) [*Nash and Sutcliffe*, 1970] from untransformed and log-transformed series. A Monte Carlo analysis was performed, in which parameter values from the manual calibration were allowed to vary by ± 20%, and the best performing parameter set was retained for scenario projections, in which the ensemble of bias corrected future climate series obtained from the 15 RCM experiments was used to project future runoff conditions.

2.5.2. Process-Based Integrated Catchment Model for Carbon (INCA-C)

INCA-C is a process-based model that simulates both terrestrial and aquatic carbon production and transport. The model requires daily time series of air temperature, precipitation, SMD, and HER (Figure 1). Terrestrial process rates are dependent on soil temperature and moisture. Soil temperature is simulated independently of DOC using routines developed for boreal conditions [*Rankinen et al.*, 2004]. Nonmonotonic relationships between soil moisture and carbon processing can be simulated, which allow maximum rates at intermediate soil wetness and slower processing when soils are excessively wet or dry.

In a nutshell, change in terrestrial DOC is simulated in INCA-C as the net rate of sorption to and desorption from soil organic carbon (SOC) minus the mass of DOC running off to surface waters. Both sorption and desorption are dependent on soil temperature and moisture ($f(T_{\mathrm{Soil}}, M)$) , and k_S and k_D represent rates of sorption and desorption, respectively. The change in mass of SOC includes additional terms for mineralization (k_M) and time-varying production from litter inputs and breakdown of plant material (p). Equations (1) and (2) present simplified representations of the changes in mass of SOC and DOC. Full descriptions of process equations are described in earlier literature [*Futter et al.*, 2007, 2009].

$$\frac{d\mathrm{DOC}}{dt} = f(T_{\mathrm{Soil}}, M)\times(k_D\times\mathrm{SOC} - k_S\times\mathrm{DOC}) - Q\times[\mathrm{DOC}] \tag{1}$$

$$\frac{d\mathrm{SOC}}{dt} = f(T_{\mathrm{Soil}}, M)\times(k_s\times\mathrm{DOC} - k_D\times\mathrm{SOC} - k_{'M}\times\mathrm{SOC}) + p \tag{2}$$

INCA-C was manually calibrated against 2005–2012 stream water [DOC] in the C2, C4, and C20 headwater catchments. The manual calibration was refined using the method of *Futter et al.* [2014] to generate a present-day INCA-C Krycklan Calibrated (KC) scenario. Model performance was assessed using NSE statistics for flow and [DOC]. For the Climate Change (CC scenarios), local-scale impacts of future climate on [DOC] were simulated by running the models with bias corrected temperature and precipitation time series (Figure 4).

2.5.3. Empirical Riparian Flow-Concentration Integration Model (RIM)

The RIM (equation (3)) assumes that stream [DOC] can be simulated as a nonlinear temperature-dependent function of runoff (equation (3)).

$$[\mathrm{DOC}] = (C_{\mathrm{base}} + k_1 \times \mathrm{T}_{\mathrm{soil}})\ \mathrm{X}(Q \times Q_o)^{(f_{\mathrm{base}} + k_2 \times T_{\mathrm{soil}})} \tag{3}$$

where C_{base} (mg L^{-1}) is baseline stream [DOC], k_1 (mg L^{-1}°C^{-1}) is the stream water concentration temperature multiplier, and T_{soil} (°C) is the soil temperature. Q is the measured runoff, Q_o (mm d^{-1}) is a calibrated runoff offset. Paramater f_{base} is the baseline flow: DOC exponent and k_2 (°C^{-1}) is an empirical temperature modifier for the flow: concentration relationship. RIM was calibrated against 2005–2012 observed stream [DOC] in the C2, C4, and C20 catchments and driven by PERSiST-simulated flow and INCA-C simulated soil temperature using the solver routine in MS-Excel to identify parameter values which minimized the sum of squared differences between simulated and observed stream [DOC] to generate a present-day Krycklan Calibrated (KC) scenario from RIM. The Climate Change (CC) scenario, in which impacts of future climate on [DOC] were evaluated, was performed by running the model with the above parameters and forcings from the 15 downscaled RCM experiments.

2.5.4. Simulation of Forestry Effects

The "Present Day Forestry" (PDF) (Table 1) results were generated in the following manner. Evidence from the Balsjö clear-cutting experiment showed increases in runoff and warmer soil temperatures following final harvesting [*Schelker et al.*, 2012]. The effects of forest harvest on runoff were simulated by adjusting parameters from the PERSiST Krycklan calibration related to snowfall, snowmelt temperature, canopy interception, and evapotranspiration so as to match the differences in runoff between the Balsjö reference and clear-cut sites

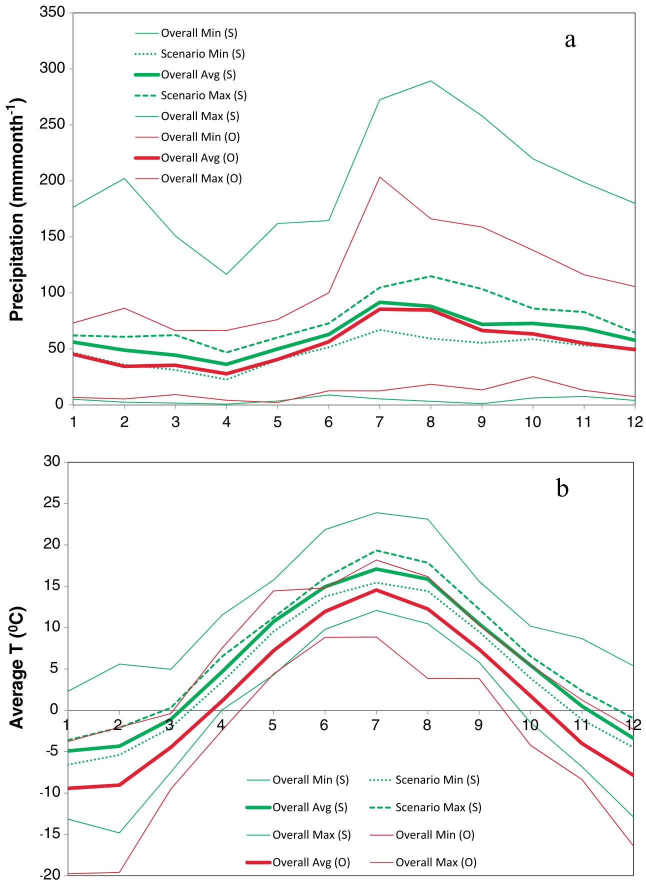

Figure 4. Summary plots of monthly precipitation (a) and average temperature (b) during the observation period (KC scenario; red lines; 1981–2012) and for the climate scenario (CC; green lines; 2061–2090). Red lines show present conditions. Thin red lines show the minimum and maximum monthly precipitation (Figure 4a) and the minimum and maximum average monthly temperature (Figure 4b). Thick red lines show average monthly precipitation and temperature. Green lines show possible future conditions based on the 15 climate scenarios. Thin green lines represent minimum and maximum monthly precipitation (Figure 4a) and the minimum and maximum average monthly temperature (Figure 4b) from the 15 scenarios. Dashed green lines represent scenario averages values. The thick dashed line represents the wettest or warmest average value from the 15 scenarios while the thin dashed line represents the driest or coldest average value.

porated to 100% harvested. While PERSiST generates daily estimates of runoff, adjustments to simulate final harvesting effects were made on a monthly basis so as to preserve the seasonal pattern in changes in runoff resulting from final harvesting. The increase in local snowfall associated with clear-felling was simulated by increasing the snow multiplier in PERSiST. This parameter scales measured precipitation to match the amount of snow accumulating in the area of interest. As a consequence of reducing canopy interception and decreasing evapotranspiration, wetter soils were simulated.

In the simulations presented here, soil temperature is simulated as a function of air temperature [*Rankinen et al.*, 2004; *Futter et al.*, 2007]. So as to reproduce the increase in soil temperature associated with forest harvesting, soil thermal conductivity parameters in INCA-C were adjusted so that simulated soil temperatures matched the observed soil temperature increase at the Balsjö clear-cut. Future local-scale forestry scenarios (FF) were simulated using downscaled climate from the 15 RCM experiments to force present-day forestry parameterizations for INCA-C, RIM, and PERSiST.

2.5.5. Combining Climate Change and Effects of Forestry at the Local Scale

Climate change (CC scenario) and forestry (PDF) effects on [DOC] (Figure 5) and fluxes (Figure 6) were first modeled separately. The Future Forestry (FF scenario) was run to assess whether or not the combined impacts of expected climate change and forest harvesting increase or reduce stream water [DOC]. By superimposing the temperature and hydrological signal of climate change and forestry effects and using these as input variables in the biogeochemical models (RIM and INCA-C), it was possible to examine the combined effects of climate change and forestry on [DOC] (Figure 7) and fluxes (Figure 8) in the future for the three landscape-element types. At the local scale, these are referred to as the “FF scenario” (Table 1).

2.5.6. Landscape-Scale Mixing Model

As noted earlier, landscape scale water quality is not merely the sum of local scale inputs. A number of scenarios were evaluated to explore the differences between local and landscape scale patterns (Table 1). Local scale outputs from the KC and PDF scenarios were used as inputs representing intact and clear-cut forests. Three scenarios were evaluated using present-day climate and differing degrees of clear-cut intensity. In the KC scenario, 0% clear-cutting was assumed while the BAU and IFH scenarios assumed 0.86% and 1.72% respectively of the landscape was clear-cut annually.

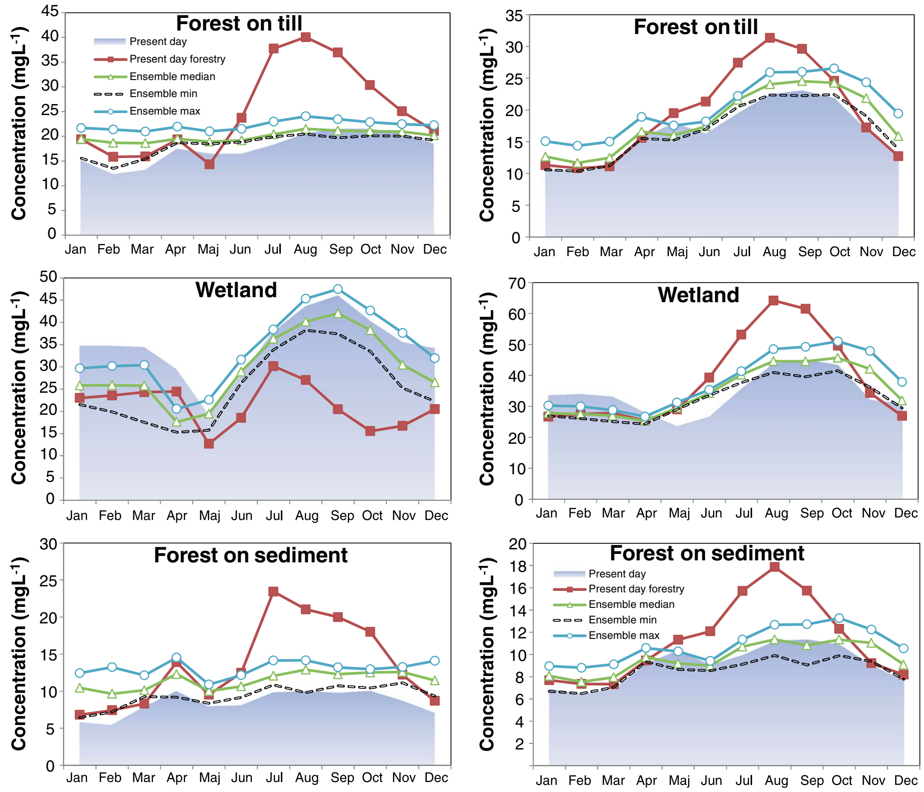

Figure 5. Local-scale simulated present-day (KC) and projected future [DOC] from (left column) INCA-C and (right column) RIM for representative boreal landscape element types showing the effects of forestry (PDF) and the possible effects of climate change (CC). Each figure shows average monthly [DOC] from the KC scenario (filled blue shapes), the PDF scenario (red line), and a summary of the CC scenario results. The black dashed line shows the lowest average [DOC] from the ensemble of 15 RCM experiments used to generate CC results, while the blue line shows the maximum of the scenario averages. The green line shows the overall scenario median value. Note the differences in scale between INCA-C and RIM simulations and between landscape element types.

All landscape scale simulations were based on *Tiwari et al.* [2014] who showed that a landscape-scale mixing model (LMM) using headwater catchments dominated by till forest, sediment forest, and wetlands landscape-element types as headwater end members (C2, C20, and C4, respectively) can be used to predict downstream concentrations by mixing local DOC signals in proportion to their areal coverage (equation (4)).

$$[\mathrm{DOC}]_s = \sum_x^3 \left(m_x \times [\mathrm{DOC}]_x\right) \quad (4)$$

where $[\mathrm{DOC}]_s$ is the landscape-scale DOC concentration in downstream surface waters, mixed from local headwater concentration signals from x identified landscape-element types (x; 1 = forest on till, 2 = wetland, 3 = forest on sediment) and m is the proportion of the areal coverage of respective landscape-element. *Tiwari et al.* [2014] also showed that by incorporating the deep groundwater flow paths into the model the RMSE improved from 5.2 mg L^{-1} to 2.2 mg L^{-1}. The magnitude of the base flow component varied as a function of discharge, f(Q), from 75% groundwater during base flow to 0% during high flow (equation (6)). In short, concentration of DOC at the outlet is a mixture of the DOC concentration signal from surface (local) and groundwater (landscape) inputs (equation (5))

$$[\mathrm{DOC}]_{\mathrm{outlet}} = p_g[\mathrm{DOC}]_g + (1\text{-}p_g)[\mathrm{DOC}]_s \quad (5)$$

where p_g is the percent of runoff from groundwater and $[\mathrm{DOC}]_g$ and $[\mathrm{DOC}]_s$ are the concentrations of DOC in groundwater and surface waters, respectively. We have been using a value of 1.25 mg L^{-1} for $[\mathrm{DOC}]_g$ based

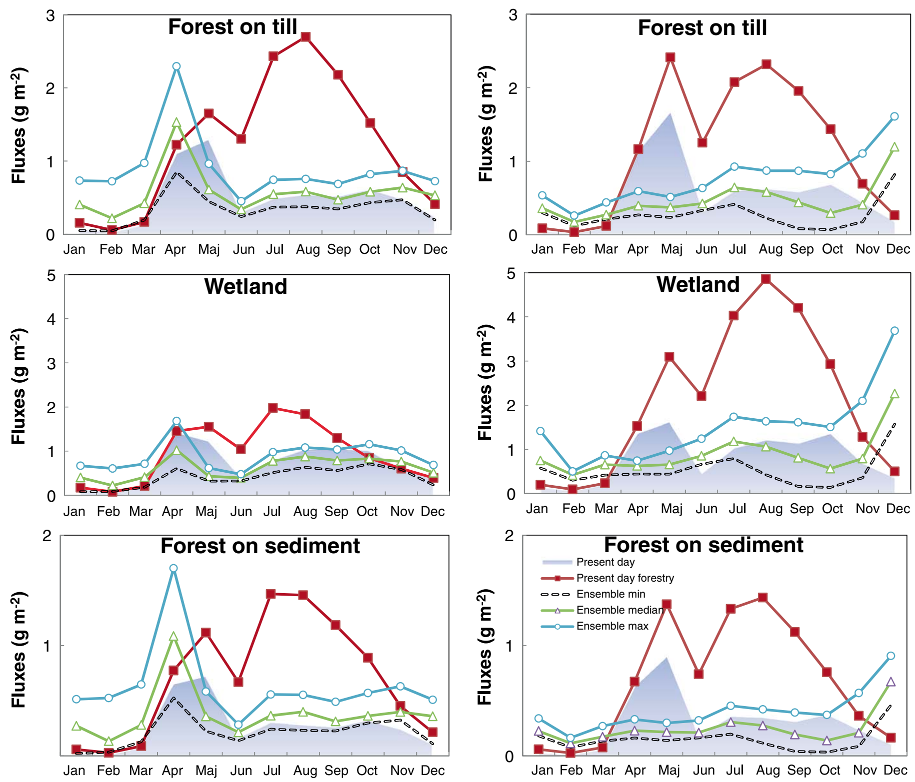

Figure 6. Local-scale simulated DOC fluxes in g DOC m^{-2} $month^{-1}$ from (left column) INCA-C and (right column) RIM for representative boreal landscape element types showing present-day conditions (KC scenario), the effects of present-day forestry (PDF) and the range of possible future climate change effects from the CC scenarios. Each figure shows average monthly DOC fluxes from the KC scenario (filled blue shapes), the PDF scenario (red line), and a summary of the CC scenario results. The black dashed line shows the lowest average DOC flux from the ensemble of 15 RCM scenarios used to generate CC results, while the blue line shows the maximum of the scenario averages. The green line shows the overall scenario median flux. Note the differences in scale between landscape element types.

on measurements from deep groundwater in a nearby well [*Tiwari et al.*, 2014]. The flow-dependent groundwater fraction in runoff was simulated using a relationship from *Tiwari et al.* [2014] (equation (6))

$$p_g = -0.139 \times \ln(r_{outlet}) + 0.3362 \quad (6)$$

where r_{outlet} is runoff at the outlet, in mm d^{-1}, and runoff is measured at C7. In the forestry scenarios (see below), runoff was adjusted to account for forestry impacts.

Landscape-scale effects of forest harvesting on DOC concentrations and fluxes (BAU and IFH scenarios; Table 1) were modeled in the following manner. The percent of the landscape affected by forestry (f) was determined based on the fraction of the landscape experiencing forestry impacts. This, in turn, was determined by the fraction harvested every year (h, % yr^{-1}), the duration of the effect (d, years), and the fraction of the local landscape-element subject to clear felling effects ($g = 1$ for forest on till and forest on sediment, 0.67 for wetlands (67% of the mires in the catchment are covered by forests)), and the fractional coverage of the different local-scale landscape-elements across the catchment (m, %)

$$f = h \times d \times \sum_{x}^{3} (m_x \times g_x) \quad (7)$$

The value of h was set to 0.86% yr^{-1} in the BAU scenario and 1.72% yr^{-1} in the IFH scenario

The effects of clear-cutting on local hydrology, soil temperature, and C biogeochemistry decline as forest cover re-establishes [*Löfgren et al.*, 2009; *Schelker et al.*, 2012]. It is assumed that the full clear-cut effect on stream water biogeochemistry is seen the first 10 years after felling and that canopy closure is reached after 30 years. The clear-cut signal is assumed to show a linear decline from total effects 10 years after felling to no

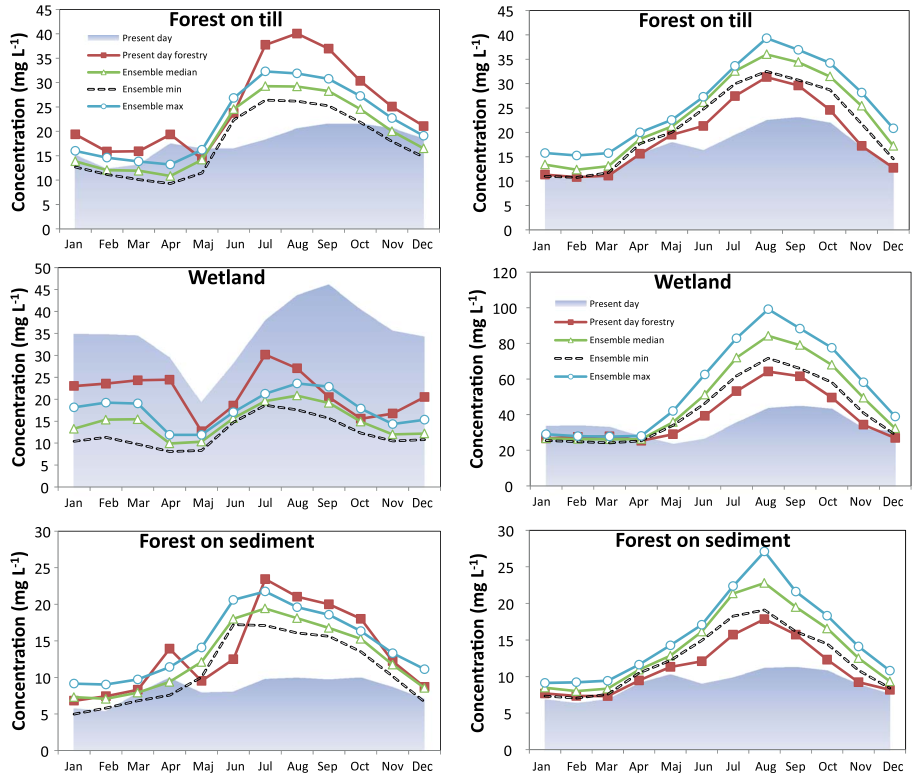

Figure 7. Local-scale simulated present-day and projected future [DOC] from (left column) INCA-C and (right column) RIM for representative boreal landscape element types showing the effects of present-day forestry (PDF) and future forestry (FF). Each figure shows average monthly [DOC] from the KC scenario (filled blue shapes), the PDF scenario (red line), and a summary of the FF scenario results where the parameterization for present-day forestry was forced with downscaled RCM outputs. The black dashed line shows the lowest average [DOC] from the ensemble of 15 RCM experiments used to generate FF results, while the blue line shows the maximum of the scenario averages. The green line shows the overall scenario median value. Note the differences in scale between INCA-C and RIM simulations and between landscape element types.

effect after 30 years. At a landscape scale, d is based on the time of 100% effect and 0.5 times the number of years for the effect to show a linear decline to zero. Thus, $d = 10 + 0.5 \times 20 = 20$ years.

Thus, r_{outlet} can be calculated as runoff from forestry affected areas plus runoff from intact forests

$$r_{\text{outlet}} = f \times r_{\text{forestry}} + (1 - f) \times r_{\text{intact}} \tag{8}$$

where r_{forestry} and r_{intact} are the simulated runoff values, in mm d^{-1}, for clear-felled and intact forests, respectively. Runoff values are obtained from PERSiST simulations.

The surface water [DOC] can be derived from the forestry and intact forest scenario [DOC] for each landscape-element. Concentrations must be prorated by runoff. Thus,

$$[\text{DOC}]_s = \left(r_{\text{intact}} \times [\text{DOC}]_{\text{intact}} + r_{\text{forestry}} \times [\text{DOC}]_{\text{forestry}}\right) / \left(r_{\text{intact}} + r_{\text{forestry}}\right) \tag{9}$$

Daily $[\text{DOC}]_{\text{intact}}$ and $[\text{DOC}]_{\text{forestry}}$ values for each landscape-element type are available from the INCA-C and RIM simulations. The surface water DOC signal at the outlet includes DOC from unharvested areas (equation (10)), plus DOC the fraction of harvested landscape-elements for which forestry effects do not apply (equation (11)) plus the DOC signal from clear-cut areas (equation (12)).

$$(1 - f) \times r_{\text{intact}} \times \sum_x^3 \left(m_x \times [\text{DOC}]_{\text{intact},x}\right) \tag{10}$$

$$f \times r_{\text{intact}} \times \sum_x^3 \left(m_x \times [\text{DOC}]_{\text{intact},x} \times (1 - g_x)\right) \tag{11}$$

$$f \times r_{\text{forestry}} \times \sum_x^3 \left(m_x \times [\text{DOC}]_{\text{forestry},x} \times g_x\right) \tag{12}$$

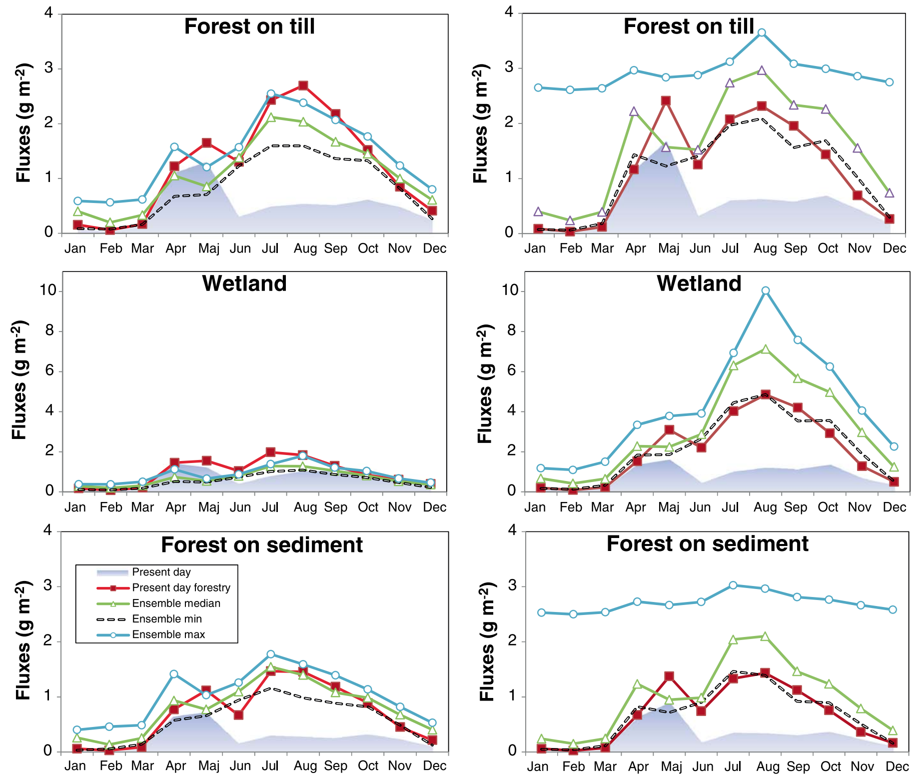

Figure 8. Local-scale simulated DOC fluxes in g DOC m^{-2} $month^{-1}$ from (left column) INCA-C and (right column) RIM for representative boreal landscape element types showing the effects of present-day forestry (PDF) and future forestry (FF). Each figure shows average monthly DOC fluxes from the KC scenario (filled blue shapes), the PDF scenario (red line), and a summary of the FF scenario results where the parameterization for present-day forestry was forced with downscaled RCM outputs. The black dashed line shows the lowest average DOC flux from the ensemble of 15 RCM scenarios used to generate FF results, while the blue line shows the maximum of the scenario averages. The green line shows the overall scenario median flux. Note the differences in scale between landscape element types.

Equations (10)–(12) must be prorated by runoff adjusted for landscape-scale forestry impacts (equation (13))

$$(1-f)\times r_{\text{intact}} + f\times r_{\text{intact}}\times \sum_x^3 (m_x\times(1\text{-}g_x)) + f\times r_{\text{forestry}}\times \sum_x^3 (m_x\times g_x) \quad (13)$$

Combining equations (10)-(13), it is possible to estimate landscape-scale DOC concentrations at the catchment outlet $[DOC]_s$:

$$[DOC]_s = ((10) + (11) + (12))/(13) \quad (14)$$

As a reference point to the scenarios we also give the present-day observed DOC. Measurements of [DOC] made at the catchment outlet (Figure 2, Site 16) were interpolated in time (2005-2012) to obtain daily values. The frequency of the measurements varies from monthly during low winter flow to 2 days-weekly during spring flood. Daily interpolated values were used to calculate a mean observed concentration and flux representative of present-day conditions.

Future landscape-scale scenarios representing climate change with no forestry (CC), "Business as Usual" forestry under a future climate (CCF) and more intensive forestry in a future climate (CCI; Table 1) were simulated in the following manner. Outputs from both RIM and INCA-C, for the three headwater landscape-elements estimated under the CC and FF scenarios, were used as inputs in the LMM to model landscape-scale DOC concentrations and fluxes at the outlet during the years 2061–2090 using the above mixing model (equation (4)). This was done so as to integrate the local-scale climate change DOC signals into possible future overall landscape-scale DOC signals.

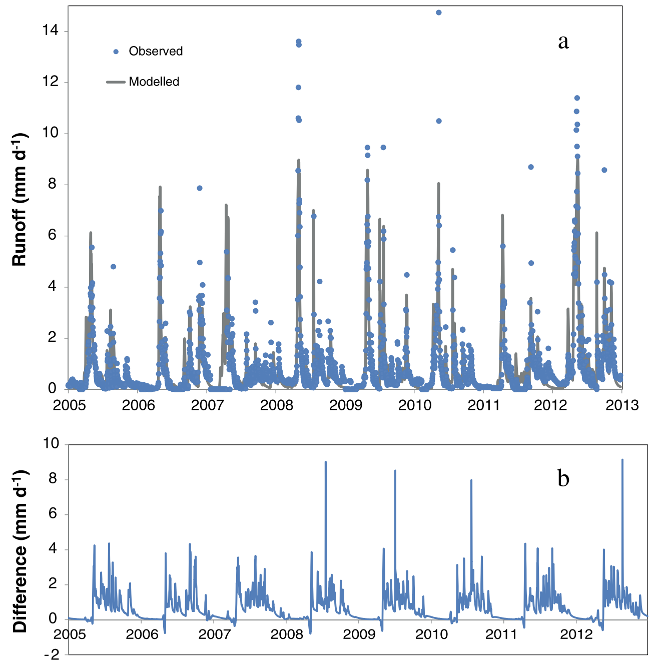

Figure 9. Plots of (a) observed (blue dots) and modeled (grey line) average daily runoff from site C7 for 2005–2012 and (b) differences between the forestry runoff scenario based on Balsjö flows (PDF; Table 1) and present-day simulations at Krycklan (KC scenario). Note that the runoff simulations were performed for 1981–2012. Only 2005–2012 results are shown for comparison with DOC results and to better display seasonal patterns. The negative spikes in Figure 9b are the result of lower snowmelt threshold temperatures in the Balsjö clear-cut scenario.

3. Results

3.1. Model Calibrations to Present-Day Conditions

The "Krycklan Calibrated" KC scenario (Table 1) includes all model calibrations to present conditions observed at Krycklan. The PERSiST model parameterization used here simulated present-day C7 streamflow with NSE values of 0.66 for both log-transformed and untransformed flows between 1981 and 2012 (Figure 9). While the total volume of runoff simulated matched observations, there are some discrepancies in summer 2011 and 2012 where precipitation measurements did not match streamflow. Between 2005 and 2012, runoff simulations captured the monthly patterns (Figure 9). However, the spring peak was, in general, slightly underestimated; summers were slightly too wet and late autumn simulations slightly too dry.

Both INCA-C and RIM were able to reproduce the short-term [DOC] dynamics in the three landscape-element types (Figure 10) with NS values of 0.30 (forest on till), 0.39 (mire), and 0.47 (forest on sediment) for INCA-C and NS values of 0.62 (forest on till), 0.57 (mire), and 0.27 (forest on sediment) for RIM. It is noteworthy that while both models had similar performance as evaluated by NS statistics, the overall patterns simulated were different, both in terms of simulated average concentrations and fluxes and temporal dynamics. This effect is most pronounced for the wetland and forest on sediment simulations. For wetlands, the INCA-C simulation did a better job of capturing the snowmelt associated DOC dilution than RIM. The INCA-C simulation for forest on sediment displays considerably more short-term variability than the RIM simulations for that landscape-element type.

3.2. Downscaled Climate Projections

Outputs from the 15 downscaled RCM experiments suggested warmer (5.5°C versus 1.8°C) and wetter (749 mm precipitation annually versus 631 mm) conditions in 2061–2090 as compared to the present day (Figure 4). Downscaled average monthly temperatures from the 15 RCM experiments were similar to the highest average monthly temperatures observed during the present day (1981–2012). Maximum monthly average temperatures are projected to be significantly warmer in all months while minimum monthly average temperatures from the 15 RCM experiments are relatively similar to the coldest monthly average temperatures under present-day conditions. The projected average monthly temperatures for 2061–2090 are similar to the maximum monthly average present-day temperatures (Figure 4).

The RCM outputs suggested that there is likely to be more precipitation in the future (Figure 4). However, the range of average monthly precipitation values projected by 15 RCM experiments was similar to average monthly present-day precipitation. There was little change in minimum monthly precipitation, but it is noteworthy that maximum future precipitation was much higher than today. There was greater variation in projected future precipitation than observed today (not shown). Projected future temperatures were less variable than under present conditions.

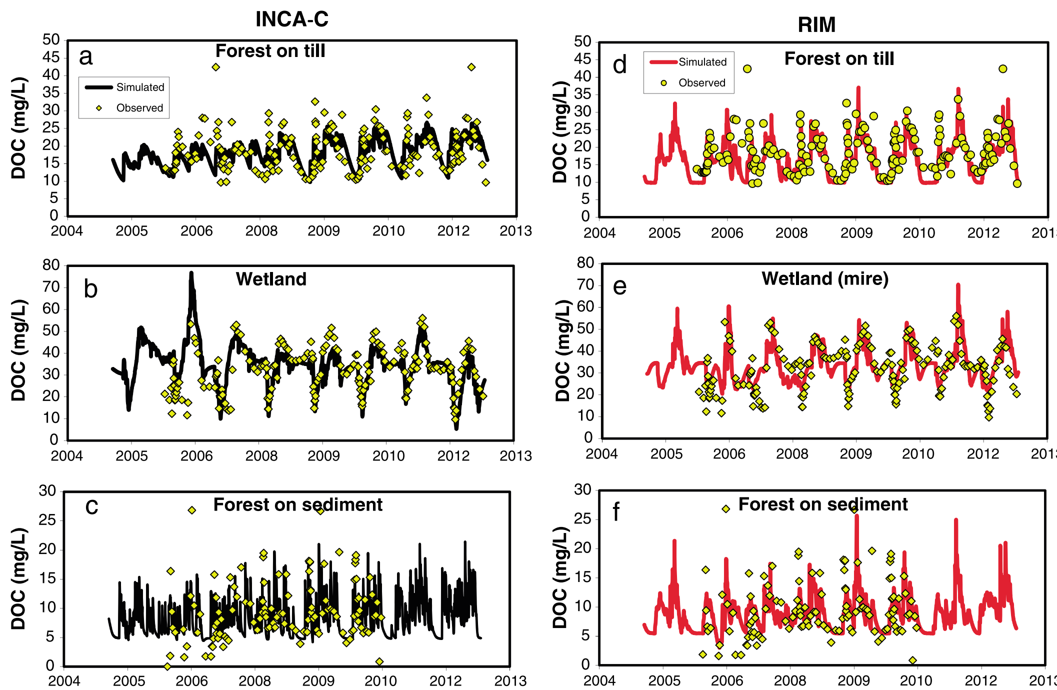

Figure 10. Results of local-scale model calibration (KC) to present-day [DOC] using (a–c) INCA-C and (d–f) RIM for landscape element types characteristic of the boreal ecozone. Solid lines represent model simulations while yellow dots are observed [DOC].

3.3. Local-Scale Present-Day Forestry Effects

The "Present-Day Forestry" PDF scenario was based on adjusting hydrological and biogeochemical model parameters from the KC scenario so as to simulate clear-cutting of the representative landscape-element types at Krycklan based on observed changes at the Balsjö clear-cut experiment. The increase in runoff observed at Balsjö following forest harvest was successfully reproduced at Krycklan in the PDF scenario (Figures 3 and 9). Winter flows were unchanged, but there was a larger spring peak associated with greater snow accumulation. Higher summer and autumn runoff were simulated as rainfall contributed to runoff instead of recharging soils, which had dried out due to evapotranspiration.

Soil thermal conductivity parameters in INCA-C were adjusted so as to match the monthly average differences in soil temperature between clear-cut and intact forest reported by *Schelker et al*. [2012] (Figure 11). INCA-C and RIM simulations were then run with the adjusted soil temperatures and hydrology from the PERSiST forestry scenario simulations. Results differed between landscape-element types and between RIM and INCA-C (Figures 5 and 6). In all cases except INCA-C wetland simulations, models simulated higher summer [DOC] (Figure 5). Winter [DOC] was similar between KC and PDF simulations in all cases, due to the lack of significant change in soil temperatures under the snowpack (Figure 11) or runoff (Figures 3 and 9). Higher DOC fluxes were simulated by both models for all landscape-element types (Figure 6). INCA-C and RIM simulated similar seasonal DOC flux patterns in both of the forest landscape-element types, with the majority of the increase occurring in summer and autumn. The largest difference in model simulations was obtained for wetlands, where INCA-C projected small flux increases associated with forest harvesting, while RIM simulated extremely high summer fluxes (Figure 6).

3.4. Local-Scale Climate Change Simulations

Local-Scale Climate Change (CC) scenario results showed that possible future climate would lead to shifts in both the timing and amount of runoff and DOC. Runoff projections under a future (2061–2090) climate (Figure 3) showed a clear shift in timing and suggested a possibility of both increases and decreases in total amount. Because of the warmer temperatures (Figure 11), higher winter flows were simulated and the spring peak was relatively smaller due to less snow accumulation and more of the total precipitation falling as rain. The smallest changes in flow between present day (KC) and under a future climate (CC) were projected for

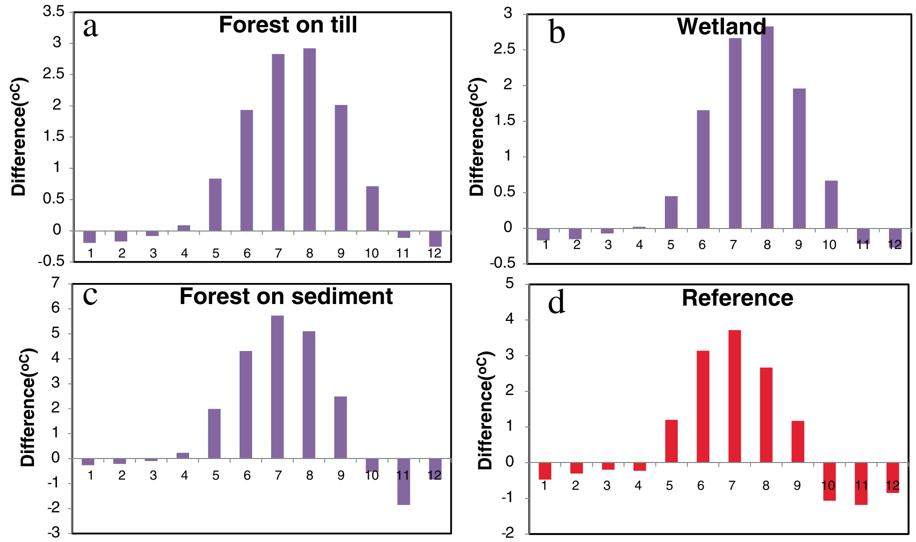

Figure 11. Plots showing the simulated average monthly deviations in soil temperature between and PDF and KC scenarios used to drive INCA-C and RIM simulations. (a–c) Based on observations of soil temperature changes after clear-cut at (d) Balsjö as reported by *Schelker et al.* [2012]. Positive values mean that the soil was warmer after clear felling while negative values represent cooler soils.

June. The minimum runoff projected from the CC scenario runs was considerably lower (192 mm yr^{-1}) than average present-day conditions (308 mm yr^{-1}), primarily due to greatly reduced spring flows. The average runoff from the 15 CC projections did not differ substantially from present-day (KC) conditions in terms of absolute amount (308 versus 314 mm yr^{-1}). The maximum runoff projected under the CC scenario (513 mm yr^{-1}) was much higher than present day with high winter flows and a pronounced snowmelt peak in April.

The simulated changes in runoff are driven by projected changes in both temperature and precipitation (Figure 4). In PERSiST, warmer temperatures result in a shift in the balance between snowfall and rain as well as higher rates of evapotranspiration (and potentially lower runoff). Higher precipitation results in increased runoff and wetter soils if it exceeds the increased evapotranspiration associated with warmer temperatures.

Both INCA-C and RIM simulated similar climate change effects on [DOC] (Figure 5). Slight increases in concentration were simulated in all cases except for INCA-C wetland simulations, where the range of projected future concentrations matched present-day conditions. Seasonal patterns of projected fluxes differed markedly between models (Figure 6). For all landscape-element types, INCA-C projected a large increase in spring DOC flux, while RIM simulations suggested that spring flux would be reduced and late autumn and winter fluxes would increase. There were only slight increases in projected summer fluxes (Figure 6).

3.5. Combined Local-Scale Effects of Climate Change and Forestry

A similar pattern to that observed for CC versus KC scenario simulations was seen when comparing the future climate change + forestry scenario (FF; Table 1) to the PDF scenario at Krycklan (Figure 3). The minimum average runoff from the 15 FF simulations (466 mm yr^{-1}) was similar to the PDF results (547 mm yr^{-1}) in all seasons except spring. The FF ensemble median runoff (645 mm yr^{-1}) was slightly higher than that for the PDF scenario, while the maximum average runoff simulated by one of the 15 FF runs was much wetter (863 mm yr^{-1}) than present-day\ observed (KC) conditions (308 mm yr^{-1}). To put these results into context, the August ensemble maximum runoff under the FF scenario is similar to the present-day spring runoff in May.

A summary of FF scenario results showing the combined possible effect of climate change and clear-cutting on stream DOC concentrations and fluxes is presented in Figures 7 and 8. In general, INCA-C simulations suggest small decreases in concentration between future and present-day clear-cuts, while RIM projections suggest increased future [DOC] as compared to present-day clear-cut impacts (Figure 7). It was only during summer months on forest on sediment land cover type that INCA-C simulations projected higher future

[DOC] than under the PDF scenario (Figure 7). The two biogeochemical models diverge in their projections of DOC dynamics in wetlands as INCA-C projected decreasing concentrations in the future while RIM projected increases. Both models projected increased DOC export from till and sediment forests, while INCA-C projected fluxes from wetlands were similar to present conditions (Figure 8).

3.6. Summary of Local Effects and Projected Landscape-Scale DOC Response

Local-scale average DOC concentrations and fluxes simulated by INCA-C and RIM under present and future conditions are presented in Figure 12, while landscape-scale results are summarized in Figure 13. When summarized at an annual scale, there were notable differences in both concentration and flux both between landscape-element types and between models (Figure 12). In general, there was good correspondence between present-day simulations and observed data for concentrations and fluxes in all landscape-element types.

For forests on till, INCA-C simulations suggested the most extreme increase in [DOC] would occur due to present-day forestry effects (PDF scenario; Figure 12a). Future [DOC] simulated under the CC and FF simulations were intermediate to present-day calibration (KC) and present-day forestry (PDF) scenario concentrations. RIM simulated concentrations for present-day forestry (PDF scenario) were within the range of climate (CC) scenario concentrations (Figure 12a). Unlike INCA-C, RIM projected the highest [DOC] for the combined climate + forestry effects (FF) in forests on till (Figure 12a).

In wetlands, INCA-C and RIM projected different directions of change in [DOC] (Figure 12b). INCA-C projected declines in [DOC] under all scenarios. The largest declines were in the climate change + forestry effects (FF), followed by present-day forestry (PDF) and climate change (CC) scenarios (Figure 12b). By contrast, RIM projected similar or increasing [DOC] under all scenarios. RIM-projected CC scenario [DOC] was not appreciably different from the present-day simulated (KC) or observed, and future forestry (FF) effects [DOC] was slightly higher than simulated for present-day forestry (PDF). RIM simulations of [DOC] under the FF were higher than any present-day observed or simulated values (Figure 12b).

INCA-C simulations of [DOC] for forests on sediment were similar to those for forests on till. The range of values projected under the climate change (CC) and climate change + forestry effects (FF) was similar and higher than present-day modeled (KC) and observed [DOC] (Figure 12c). Forestry effect simulations displayed high interannual variability in [DOC] and spanned a similar concentration range to that of the climate scenarios. The RIM simulations for sediment forests presented a [DOC] pattern more similar to RIM simulated [DOC] from wetlands. Projected [DOC] under the climate scenarios (CC) was similar to present-day concentrations, and forestry effects [DOC] was intermediate to the range of values simulated in the CC and FF scenarios (Figure 12c). An important finding was that on the local scale (Figure 12) the combined effects of climate change and forestry effects on [DOC] were not additive.

INCA-C simulated increased DOC fluxes from both till and sediment forests (Figures 12d and 12f) under both climate change (CC) and future forestry (FF) scenarios. For both forest types, INCA-C projected slight flux increases under a changing climate (CC) and a large increase under the climate change + forestry effects scenarios (FF). In both cases, projected DOC fluxes for forestry effects were similar to values simulated for climate change + forestry effects (Figures 12d and 12f). Very little change in flux from wetlands was simulated by INCA-C for any of the climate scenarios (Figure 12e).

RIM simulated similar fluxes for till forests and wetlands (Figures 12d and 12e). Present-day (KC) fluxes were similar to those under the CC scenario. The largest flux and most variable flux increases were projected for FF scenario. Simulated present-day forestry (PDF scenario) fluxes were intermediate to CC and FF fluxes. For forests on sediment, RIM projected a slightly smaller increase in flux for the PDF scenario than for either CC or FF scenarios.

When the individual landscape-element type responses were integrated across a larger catchment using the LMM a different pattern emerged (Figure 13). Observed average [DOC] at the Krycklan outlet was 9.9 mg L^{-1}, which was in between the KC scenarios which assumed no clear-cuts (8.9 and 9.0 mg L^{-1} for INCA-C and RIM) and the present-day BAU scenarios (10.0 and 10.4 mg L^{-1} for INCA-C and RIM, respectively). This is to be expected since approximately 25% of the Krycklan catchment has been protected from harvesting since 1922 [*Laudon et al.*, 2013a] and the catchment as a whole therefore should have a smaller DOC signal from

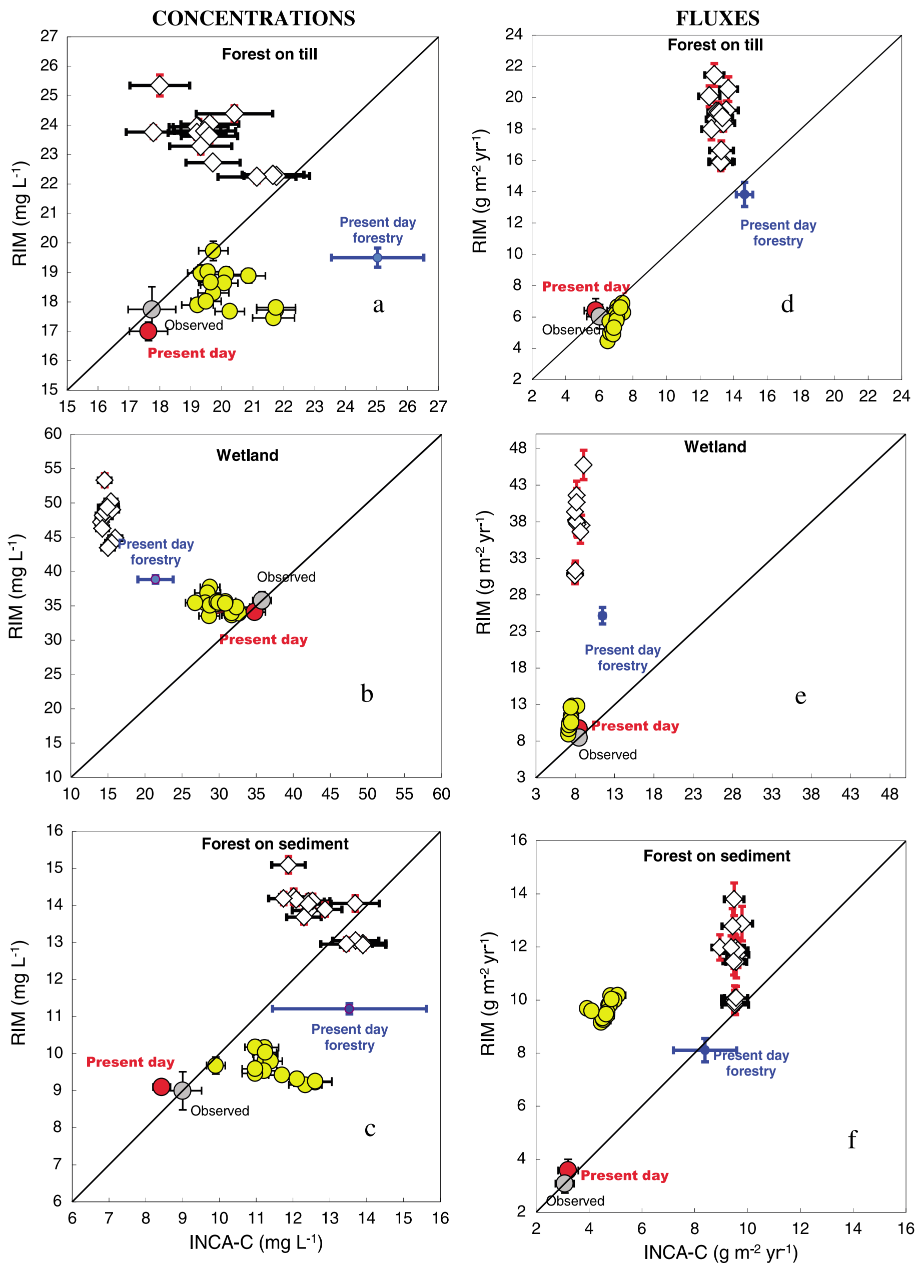

Figure 12. Summary of present-day (KC and PDF) and projected future (CC and FF) local-scale INCA-C (horizontal axis) and RIM (vertical axis) simulations showing annual average (left column) DOC concentrations and (right column) fluxes for forest on (a and d) till, (b and e) wetland, and (c and f) forest on sediment. Lengths of the bars on the crosses show standard errors of the annual values. Grey dots represent average observed concentrations and fluxes between 2005 and 2012. Red dots show present-day calibrated values from the KC scenario. The blue cross represents values from the PDF scenario. Yellow dots represent the average values from each of the 15 RCM forcings in the CC scenario. White diamonds show the results of individual RCM forcings in the future forestry (FF) scenario. Note that the effects of climate change and forestry are not additive. If effects were additive, projections would move upwards along the diagonal instead of displaying the trajectories presented here.

forestry than the average forest landscape in Sweden that was considered in the BAU scenarios. A range of average concentrations between 9.3 and 11.3 mg L^{-1} was projected for the CC scenario, in which there were no clear-cuts simulated. The average INCA-C projected concentration (10.6 mg L^{-1}) was slightly higher than that projected by RIM (10.2 mg L^{-1}). For the future "Business As Usual" (CCF) scenario, a range of annual average [DOC] between 10.5 and 13.3 mg L^{-1} was projected. The average INCA-C projected concentration

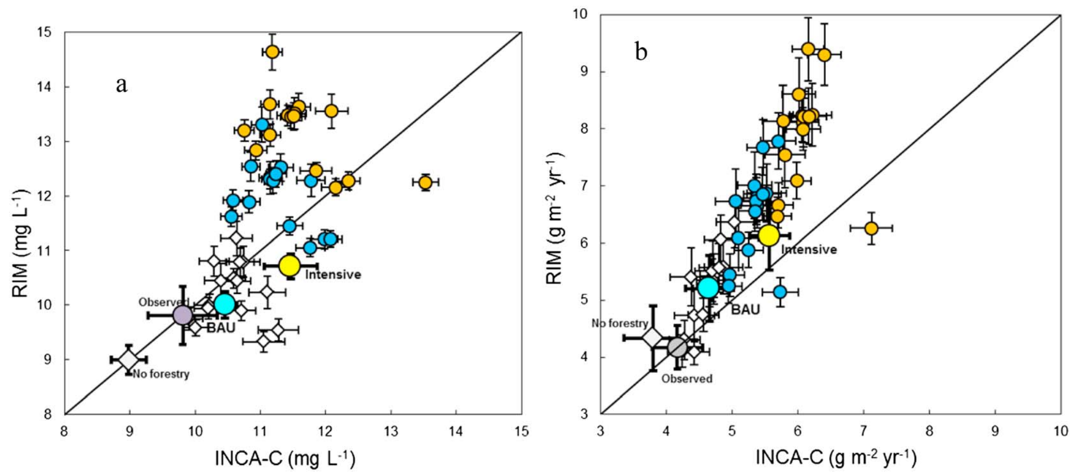

Figure 13. Present day (KC, BAU, and IFH scenarios) and potential future (CC, CCF, and CCI scenarios) landscape-scale annual average (a) DOC concentrations and (b) fluxes from INCA-C (horizontal axis) and RIM (vertical axis) as simulated the Landscape Mixing Model at the Krycklan catchment outlet. The bars on the crosses show standard errors of the mean values. Observed values are represented using a grey circle. The two landscape scale, present-day forestry scenarios are shown as light blue circles (BAU) and bright yellow circles (IFH). The points labeled "No Forestry" represent the upscaled KC scenario assuming no clear-cutting in the catchment. White diamonds represent individual RCM forcings under the CC scenario which assumes no clear-cutting and a changing climate. Dark blue dots represent individual RCM forcings under the CCF climate change and business as usual forestry scenario (0.86 % of the catchment harvested annually), while dark yellow dots represent individual RCM forcings under the CCI climate change and intensive (2X business as usual) forest harvest scenario. At the landscape scale, effects of forestry and are additive as the scenario realizations move approximately along the diagonal as the intensity of forest harvest increases.

(11.3 mg L^{-1}) was lower than that projected by RIM (12.0 mg L^{-1}). Higher average concentrations were projected under the more intensive forest harvesting (CCI scenario; 10.8 to 14.6 mg L^{-1}), the average INCA-C projected concentration was substantially lower than the RIM estimate (11.6 versus 13.2 mg L^{-1}).

The pattern of modeled and observed fluxes (Figure 13b) was harder to interpret. The observed flux (4.2 g m^{-2} yr^{-1}) was more similar to the KC scenario, which assumed no clear-cuts (3.8 and 4.3 g m^{-2} yr^{-1} for INCA-C and RIM, respectively) than it was to the present-day BAU (4.7 and 5.2 g m^{-2} yr^{-1} for INCA-C and RIM, respectively) or IFH scenarios (5.6 and 6.1 g m^{-2} yr^{-1} for INCA-C and RIM). Projected future fluxes showed a similar pattern to concentrations, increasing forest harvest intensity led to higher fluxes. Under the CC scenario, which assumed 0% clear-cut, a range of average fluxes between 4.1 and 6.4 g m^{-2} yr^{-1} was projected. The range of RIM projected values (2.3 g m^{-2} yr^{-1}) was higher than the range of INCA-C projections (0.8 g m^{-2} yr^{-1}), and the average RIM projected value was higher than that obtained using INCA-C (5.2 versus 4.6 g m^{-2} yr^{-1}). Similar behaviors were seen for the two climate change + forestry scenarios. Under the CCF scenario, projected fluxes ranged between 5.0 and 7.8 g m^{-2} yr^{-1}. The range of RIM projections (2.7 g m^{-2} yr^{-1}) was higher than those for INCA-C (0.8 g m^{-2} yr^{-1}), and the average RIM projected value was higher than that from INCA-C simulations (6.5 versus 5.3 g m^{-2} yr^{-1}). Under the more intensive forestry CCI scenario, projected fluxes ranged between 5.7 and 9.4 g m^{-2} yr^{-1}. The range of RIM projections (3.1 g m^{-2} yr^{-1}) was higher than those for INCA-C (1.4 g m^{-2} yr^{-1}) and the average RIM projected value was higher than that from INCA-C simulations (7.9 versus 6.1 g m^{-2} yr^{-1}).

An interesting result was that when the individual landscape-element type responses (Figure 12) were integrated across a larger catchment to the landscape scale a different pattern emerged where the combined signal of climate change + forestry effects went from not being additive to mostly being additive (Figure 13).

4. Discussion

Many studies have shown the vulnerability of boreal forest aquatic ecosystems to climate change impacts [*Bonan*, 2008; *Davidson and Janssens*, 2006; *Laudon et al.*, 2012, 2013b; *Nabuurs et al.*, 2013; *Tetzlaff et al.*, 2013] and the impacts of forest harvesting on surface water quality [*Kreutzweiser et al.*, 2008; *Laudon et al.*, 2011b; *Palviainen et al.*, 2014; *Schelker et al.*, 2012, 2013a, 2014]. To date, there has been limited evaluation of the combined impact of these two stressors on water quality in the boreal forest. Uncertainties associated with the possible effects of multiple stressors on boreal water resources can be evaluated by the use of ensembles of climate scenarios and multiple models of biogeochemical processes. However, the huge range of sources of uncertainty including (but not limited to) emissions scenario, GCM representation of climate processes, downscaling technique, data availability, model lack of fit, and model structural and parameter uncertainty makes it impossible to perform a full uncertainty analysis. In light of this limitation, this study presents simulations of possible future water quality at local and landscape scales under a range of climate and forest harvest scenarios for use in storylines, or internally consistent descriptions of plausible futures.

4.1. Hydrological Responses

Adequate hydrological simulations are needed for catchment biogeochemical modeling. The simulations presented here were able to capture the pattern of hydrological response at the C7 gauging site downstream of the forest on till (C2) and wetland (C4) headwater catchments. It should be noted that relying on one parameter set realization from a single rainfall-runoff model introduces uncertainties in the projection of future conditions. Specifically, climate change effects on evapotranspiration are still inadequately understood [*Watts et al*., 2015]. Using multiple model runs with a range of values for parameters related to evapotranspiration would result in an improved representation of uncertainties, but would require significant computer resources.

Parameter values related to effects of clear-cuts were adjusted so as to reproduce the forest harvesting effect observed at the nearby Balsjö catchment. There has been a large number of paired catchment studies in Sweden [*Futter et al*., 2010] and elsewhere [*Brown et al*., 2005] documenting the effects of forest harvesting on runoff. While the general trend toward increasing summer runoff is apparent in almost all studies, the exact magnitude of effects varies. Balsjö is the closest operational study for which data are available during the calibration period used here. Some uncertainty has been introduced into the results presented here as it was assumed that Krycklan C7 runoff is representative of boreal Swedish headwaters and that hydrological response at Balsjö would have been observed at other clear-cuts. Unfortunately, the necessary data are not currently available to conclusively test these hypotheses.

At a landscape scale, simulations suggested a slight increase in runoff associated with forest harvesting, mostly during the growing season. This is consistent with another study from north eastern Ontario where moderate increases in low flows in medium to large rivers with different degrees of forest harvest intensity were reported [*Buttle and Metcalfe*, 2000].

When using meteorological data from the RCM experiments to drive the rainfall-runoff model, a shift in spring melt regimes due to shortened and warmer winters was simulated (Figures 3 and 4). This is consistent with other climate change impact studies in the boreal forest [*Holmberg et al*., 2014; *Oni et al*., 2014; *Thorne*, 2011; *Woo et al*., 2008]. The general trend toward slight increases in future precipitation is also consistent with other studies [*Chen et al*., 2015].

4.2. Calibrating Local-Scale Biogeochemical Models

There are a number of approaches to modeling [DOC] including neural network [*Aitkenhead-Peterson et al*., 2005; *Aitkenhead et al*., 2007], process-based [*Futter et al*., 2007; *Naden et al*., 2010; *Wu et al*., 2014], and empirical [*Hejzlar et al*., 2003; *Herrmann et al*., 2015; *Temnerud et al*., 2014] approaches. The use of two models in the simulations presented here should not be construed as spanning the range of modeling possibilities, but is more akin to "getting a second opinion" from the medical profession.

Both RIM and INCA-C were able to simulate seasonal and long term patterns in present-day [DOC] at each of the headwater sites (Figure 10). RIM simulations had better goodness of fit statistics than were obtained produced using INCA-C. This is not surprising as empirical regression models almost always produce simulations with smaller residuals than can be obtained using process-based models [*Futter and de Wit*, 2008]. The differences between INCA–C and RIM scenario projections are related to model structure. RIM is a nonlinear regression model which simulates monotonic responses to soil temperature and runoff. Thus, it can give more extreme projections than obtained by INCA-C, which simulates both production and consumption of DOC, and is therefore able to simulate both positive and negative responses to the same environmental forcing. This means that the INCA-C model structure is consistent with *Laudon et al*. [2012], who suggest that [DOC] displays a modal response to temperature with concentrations increasing up to a point and then declining with further warming.

While empirical models such as RIM are, in general, easier to apply and produce better goodness of fit statistics than process-based models such as INCA-C, their use in scenarios is problematic. Empirical models are developed using correlative patterns, and thus reflect current relationships between dependent and independent variables [*Crossman et al*., 2014]. If these relationships do not hold in the future, empirical models will give spurious results [*Leavesley*, 1994]. On the other hand, process-based models such as INCA-C have a greater focus on representing the underlying biogeochemical and physical processes that describe system behavior [*Adams et al*., 2012; *Crossman et al*., 2014]. As model parameters have a specific physical meaning, which can be defined for future altered conditions, process-based models such as INCA-C can be applied with more confidence outside the range of data under which they were developed, and hence have a greater ability to deliver credible projections under possible future conditions [*Leavesley*, 1994; *Crossman et al*., 2014].

4.3. Climate Change and Forestry Impacts on DOC in the Local Scale

Boreal forest landscapes are made up of distinct landscape elements with unique biogeochemical signatures. This heterogeneity results in complex biogeochemical responses across the spatial gradient from local to landscape scale in large catchments [*Löfgren et al*., 2009; *Schelker et al*., 2014; *Sørensen et al*., 2009a]. Whereas warmer and wetter soils associated with a changing climate and forest harvesting often enhance DOC production and transport [*Hongve et al*., 2004; *Öquist et al*., 2014; *Tipping et al*., 1999], it is unclear whether the combined impacts of climate change and forest harvesting will increase or reduce stream [DOC] due to uncertainties associated with landscape heterogeneity, hydrologic connectivity, incomplete process understanding, and other local or regional influences [*Clark et al*., 2010]. In this study, we modeled the effects of climate change only and forestry effects only (Figures 5 and 6), but also the combined effect of climate change and forestry (Figures 7, 8, and 12). Combined climate and forestry effects were assessed by incorporating the hydrological and temperature change signals associated with clear-cutting into the parameterizations used to drive the hydrological and biogeochemical models, thereby allowing them to interact and give a combined DOC signal. Both climate change and forestry lead to changes in timing of flow and amount of runoff. On their own, climate change leads to earlier, smaller spring peaks and clear-cuts promote sustained summer base flow. The combined effects of climate change and forestry will be unprecedented in terms of their wetness. This will almost certainly impact soil processes and hence [DOC]. At a local scale the combined signals from climate change and forestry was not additive, suggesting that there are complex, nonlinear interactions between them that affect the stream biogeochemistry of headwaters draining different landscape elements. However, when aggregated to the landscape scale this pattern disappeared and the diversified signals from the landscape-elements combined into a general signal from the forest landscape that was mostly additive (Figure 13).

The assumed duration of harvest effects adds additional uncertainty to the results presented here. The long-term modeled impact of forestry on stream DOC is highly dependent on the duration of increased [DOC] following a harvest; it is also important to support long-term monitoring studies, which evaluate the mechanisms and duration of increased mobilization of DOC after clear-cutting. Recent studies suggest that fluvial DOC responses will result from forestry-induced hydrologic changes/flow paths as a primary driver, but that the higher soil temperature, which control biogeochemical process and transpiration rates, may also contribute [*Palviainen et al*., 2014; *Schelker et al*., 2013b].

4.4. Fluvial Carbon Responses at the Landscape Scale and Environmental Implications for the Future

This study is a modeling exercise, in which regional climate change models were linked to hydrological and biogeochemical models so as to simulate local water chemistry, which is then mixed in a landscape mixing model to provide overall landscape DOC concentration and export scenarios for the whole boreal forest landscape. Environmental modeling always encompasses uncertainties; one way of addressing this is to use an ensemble modeling approach. Using an ensemble of multiple models makes explicit the existence of uncertainty, but it does not set quantitative bounds on the full range of future possibilities. Instead, the model outputs presented here should be treated as multiple plausible outcomes or scenario storylines [*Börjeson et al*., 2006; *Milestad et al*., 2014; *Rounsevell and Metzger*, 2010], which can assist decision making. This is analogous to how Intergovernmental Panel on Climate Change uses scenario storylines to present possible effects of climate change.

Previous research works on critical harvesting thresholds suggest that at least 11% of a catchment needs to be clear-cut in order for a significant ($p < 0.05$) increase in DOC concentrations can be detected in downstream larger stream reaches [*Schelker et al.*, 2014]. In the BAU scenario 0.86% was clear-cut annually and the effects were assumed to last 20 years, which means that on average 17% of the catchment could be considered to be affected by forest harvesting at all times. Thus, it is not surprising that a clear signal of forestry effects on [DOC] was simulated.

There are a number of possible explanations for the additivity of climate and forestry effects at the landscape scale. Wetlands cover a relatively small amount (9%) of the catchment; thus, their influence will be relatively minor at the landscape scale and their local-scale nonadditivity will be hard to detect. The local-scale forest on till and forest on sediment [DOC] projections are similar and closer to additive. Because they are the dominant land cover types in the catchment, they will drive landscape-scale concentration inputs. Runoff is additive across scenarios and this will tend to make fluxes additive. Furthermore, any differences in land-cover specific concentrations are masked by the homogeneous groundwater inputs assumed for all scenarios.

Although the responses to the future scenarios differed between different landscape units, the overall signal from the whole forest landscape is probably the most important result as this is what affects the downstream lakes and rivers. If the modeling results presented here hold true, then climate change can be expected to increase DOC concentrations in stream water draining the forest landscape in the future in the order of 1 mg L^{-1} (Figure 13). Add to this 1 mg L^{-1}, (approximately 10%) driven by effects of forestry and if forestry will intensify in the future an additional 1 mg L^{-1} (Figure 13). The results from the storyline scenarios in this study also showed that DOC fluxes from the forest landscape could increase in the future, from somewhere around a 50% increase to in the worst-case scenarios doubling, in the upcoming 75 years. This might affect the carbon balance of the forest landscape as much of the carbon that enters into a stream network is quickly released back into the atmosphere. This vertical CO_2 flux can make up 50% of the entire stream flux [*Wallin et al.*, 2013]. Between 30 and 80% of the carbon entering into Scandinavian freshwater system has been shown to be lost in lakes through sedimentation and mineralization before reaching the Baltic Sea [*Algesten et al.*, 2004]. This still means that 20–70% of the increased loadings are likely to reach the sea. The brownification of surface waters and coastal waters suggested in this study will most likely affect the nutrient status and light regime and shift food webs toward net heterotrophy [*Andersson et al.*, 2013; *Wikner and Andersson*, 2012]. While eutrophication is one of the major environmental concerns for the Baltic Sea [*Karlson et al.*, 2002; *Saikku and Asmala*, 2010], increasing fluxes of DOC which acts as a transport vector for nutrients [*Stepanauskas et al.*, 2002], metals, and persistent organic pollutants [*Bergknut et al.*, 2010] may also harm Baltic ecosystem health.

5. Conclusion

No one can predict exactly what will happen in the future, but, by using a set of plausible and internally consistent scenarios and different models, we can constrain uncertainties about the future. So while all scenarios give different results and while the results of this study cannot be verified until 2090, these modeling exercises can be used to explore plausible possible futures and to guide decision-making in Sweden and elsewhere. This is the first study in which the combined impact of climate change and forestry effects on boreal stream biogeochemistry has been assessed. The combined impacts of expected climate change and forest harvesting on DOC concentrations and fluxes indicated complex interactive processes on the local scale as the results were not additive. However, when aggregating to the landscape scale the results were found to be mostly additive and both forestry and climate change will increase DOC concentrations and fluxes in large-scale boreal surface waters. While the average projected magnitude of any increase in [DOC] is less than that already observed in many boreal waterbodies recovering from acidification, the plausible increases in DOC flux may have negative impacts on the Baltic Sea.

Acknowledgments
This project was funded by two larger projects ForWater and Future Forest, studying the effect of climate and forest managements on boreal water resources. More information about the data used in this study is available in *Laudon et al.* [2013a] or can be requested at http://www.slu.se/en/departments/forest-ecology-management/research/krycklan-catchment-study-new/dataservice/. Funding for KCS came from Swedish Science Council (SITES), Formas (ForWater), SKB, MISTRA (Future Forest), and Kempe Foundation. The ENSEMBLES data used in this work (http://ensembles-eu.metoffice.com/docs/Ensembles_final_report_Nov09.pdf) were funded by the EU FP6 Integrated Project ENSEMBLES (Contract number 505539), whose support is gratefully acknowledged. M.N.F. acknowledges the support of the NordForsk DomQua project. The comments of two anonymous reviewers greatly improved the quality of the final manuscript.

References

Adams, H. D., A. P. Williams, C. Xu, S. A. Rauscher, X. Jiang, and N. G. McDowell (2012), Empirical and process-based approaches to climate-induced forest mortality models, *Front. Plant Sci.*, *4*, 438–438.

Ågren, A., I. Buffam, M. Jansson, and H. Laudon (2007), Importance of seasonality and small streams for the landscape regulation of dissolved organic carbon export, *J. Geophys. Res.*, *112*, G03003, doi:10.1029/2006JG000381.

Ågren, A., I. Buffam, D. Cooper, T. Tiwari, C. Evans, and H. Laudon (2014), Can the heterogeneity in stream dissolved organic carbon be explained by the contributing landscape elements?, *Biogeosciences*, *11*(4), 1199–1213.

Aitkenhead, M., J. Aitkenhead-Peterson, W. McDowell, R. Smart, and M. Cresser (2007), Modelling DOC export from watersheds in Scotland using neural networks, *C. R. Geosci.*, *33*(3), 423–436.

Aitkenhead-Peterson, J., J. Alexander, and T. Clair (2005), Dissolved organic carbon and dissolved organic nitrogen export from forested watersheds in Nova Scotia: Identifying controlling factors, *Global Biogeochem. Cycles*, *19*, GB4016, doi:10.1029/2004GB002438.

Algesten, G., S. Sobek, A. K. Bergström, A. Ågren, L. J. Tranvik, and M. Jansson (2004), Role of lakes for organic carbon cycling in the boreal zone, *Global Change Biol.*, *10*(1), 141–147.

Andersson, A., I. Jurgensone, O. F. Rowe, P. Simonelli, A. Bignert, E. Lundberg, and J. Karlsson (2013), Can humic water discharge counteract eutrophication in coastal waters?, *PLoS One*, *8*(4e61293), doi:10.1371/journal.pone.0061293.

Apps, M., W. Kurz, R. Luxmoore, L. Nilsson, R. Sedjo, R. Schmidt, L. Simpson, and T. Vinson (1993), Boreal forests and tundra, *Water Air Soil Pollut.*, *70*(1-4), 39–53.

Aufdenkampe, A. K., E. Mayorga, P. A. Raymond, J. M. Melack, S. C. Doney, S. R. Alin, R. E. Aalto, and K. Yoo (2011), Riverine coupling of biogeochemical cycles between land, oceans, and atmosphere, *Front. Ecol. Environ.*, *9*(1), 53–60.

Battin, T. J., S. Luyssaert, L. A. Kaplan, A. K. Aufdenkampe, A. Richter, and L. J. Tranvik (2009), The boundless carbon cycle, *Nat. Geosci.*, *2*(9), 598–600.

Bergknut, M., S. Meijer, C. Halsall, A. Ågren, H. Laudon, S. Köhler, K. C. Jones, M. Tysklind, and K. Wiberg (2010), Modelling the fate of hydrophobic organic contaminants in a boreal forest catchment: A cross disciplinary approach to assessing diffuse pollution to surface waters, *Environ. Pollut.*, *158*(9), 2964–2969.

Bonan, G. B. (2008), Forests and climate change: Forcings, feedbacks, and the climate benefits of forests, *Science*, *320*(5882), 1444–1449.

Börjeson, L., M. Höjer, K.-H. Dreborg, T. Ekvall, and G. Finnveden (2006), Scenario types and techniques: Towards a user's guide, *Futures*, *38*(7), 723–739.

Brown, A. E., L. Zhang, T. A. McMahon, A. W. Western, and R. A. Vertessy (2005), A review of paired catchment studies for determining changes in water yield resulting from alterations in vegetation, *J. Hydrol.*, *310*(1), 28–61.

Buttle, J., and R. Metcalfe (2000), Boreal forest disturbance and streamflow response, northeastern Ontario, *Can. J. Fish. Aquat. Sci.*, *57*(S2), 5–18.

Chen, D., C. Achberger, T. Ou, U. Postgård, A. Walther, and Y. Liao (2015), Projecting future local precipitation and its extremes for Sweden, *Geogr. Ann. Ser. A Phys. Geogr.*, *97*(1), 25–39.

Christiansen, L. (2014), *Swedish Statistical Yearbook of Forestry*, 363 pp., Swedish For. Agency, Jönköping, Sweden.

Clark, J., S. Bottrell, C. Evans, D. Monteith, R. Bartlett, R. Rose, R. Newton, and P. Chapman (2010), The importance of the relationship between scale and process in understanding long-term DOC dynamics, *Sci. Total Environ.*, *408*(13), 2768–2775.

Cole, J. J., Y. T. Prairie, N. F. Caraco, W. H. McDowell, L. J. Tranvik, R. G. Striegl, C. M. Duarte, P. Kortelainen, J. A. Downing, and J. J. Middelburg (2007), Plumbing the global carbon cycle: Integrating inland waters into the terrestrial carbon budget, *Ecosystems*, *10*(1), 172–185.

Cooper, D., A. Jenkins, R. Skeffington, and B. Gannon (2000), Catchment-scale simulation of stream water chemistry by spatial mixing: Theory and application, *J. Hydrol.*, *233*(1), 121–137.

Crossman, J., M. N. Futter, P. G. Whitehead, E. Stainsby, H. M. Baulch, L. Jin, S. K. Oni, R. L. Wilby, and P. J. Dillon (2014), Flow pathways and nutrient transport mechanisms drive hydrochemical sensitivity to climate change across catchments with different geology and topography, *Hydrol. Earth Syst. Sci.*, *18*(12), 5125–5148.

Cui, X., S. Liu, and X. Wei (2012), Impacts of forest changes on hydrology: A case study of large watersheds in the upper reaches of Minjiang River watershed in China, *Hydrol. Earth Syst. Sci.*, *16*(11), 4279–4290.

Davidson, E. A., and I. A. Janssens (2006), Temperature sensitivity of soil carbon decomposition and feedbacks to climate change, *Nature*, *440*(7081), 165–173.

Déqué, M., D. Rowell, D. Lüthi, F. Giorgi, J. Christensen, B. Rockel, D. Jacob, E. Kjellström, M. De Castro, and B. van den Hurk (2007), An intercomparison of regional climate simulations for Europe: Assessing uncertainties in model projections, *Clim. Change*, *81*(1), 53–70.

Egnell, G., H. Laudon, and O. Rosvall (2011), Perspectives on the potential contribution of Swedish forests to renewable energy targets in Europe, *Forests*, *2*(2), 578–589.

Ehret, U., E. Zehe, V. Wulfmeyer, K. Warrach-Sagi, and J. Liebert (2012), HESS Opinions "Should we apply bias correction to global and regional climate model data?", *Hydrol. Earth Syst. Sci.*, *16*(9), 3391–3404.

Futter, M., D. Butterfield, B. Cosby, P. Dillon, A. Wade, and P. Whitehead (2007), Modeling the mechanisms that control in-stream dissolved organic carbon dynamics in upland and forested catchments, *Water Resour. Res.*, *43*, W02424, doi:10.1029/2006WR004960.

Futter, M., M. Forsius, M. Holmberg, and M. Starr (2009), A long-term simulation of the effects of acidic deposition and climate change on surface water dissolved organic carbon concentrations in a boreal catchment, *Hydrol. Res.*, *40*, 291–305.

Futter, M., E. Ring, L. Högbom, S. Entenmann, and K. Bishop (2010), Consequences of nitrate leaching following stem-only harvesting of Swedish forests are dependent on spatial scale, *Environ. Pollut.*, *158*(12), 3552–3559.

Futter, M., S. Löfgren, S. Köhler, L. Lundin, F. Moldan, and L. Bringmark (2011), Simulating dissolved organic carbon dynamics at the Swedish integrated monitoring sites with the integrated catchments model for carbon, INCA-C, *Ambio*, *40*(8), 906–919.

Futter, M., M. Erlandsson, D. Butterfield, P. Whitehead, S. Oni, and A. Wade (2014), PERSiST: A flexible rainfall-runoff modelling toolkit for use with the INCA family of models, *Hydrol. Earth Syst. Sci.*, *10*, 8635–8681.

Futter, M. N., and H. A. de Wit (2008), Testing seasonal and long-term controls of streamwater DOC using empirical and process-based models, *Sci. Total Environ.*, *407*(1), 698–707.

Grabs, T., K. Bishop, H. Laudon, S. W. Lyon, and J. Seibert (2012), Riparian zone hydrology and soil water total organic carbon (TOC): Implications for spatial variability and upscaling of lateral riparian TOC exports, *Biogeosciences*, *9*(10), 3901–3916.

Hagedorn, F., S. Patrick, W. Peter, and F. Hannes (2000), Export of dissolved organic carbon and nitrogen from Gleysol dominated catchments—The significance of water flow paths, *Biogeochemistry*, *50*(2), 137–161.

Hejzlar, J., M. Dubrovský, J. Buchtele, and M. Růžička (2003), The apparent and potential effects of climate change on the inferred concentration of dissolved organic matter in a temperate stream (the Malše River, South Bohemia), *Sci. Total Environ.*, *310*(1), 143–152.

Herrmann, M., R. G. Najjar, W. M. Kemp, R. B. Alexander, E. W. Boyer, W. J. Cai, P. C. Griffith, K. D. Kroeger, S. L. McCallister, and R. A. Smith (2015), Net ecosystem production and organic carbon balance of US East Coast estuaries: A synthesis approach, *Global Biogeochem. Cycles*, *29*, 96–111, doi:10.1002/2013GB004736.

Holmberg, M., M. N. Futter, N. Kotamäki, S. Fronzek, M. Forsius, P. Kiuru, N. Pirttioja, K. Rasmus, M. Starr, and J. Vuorenmaa (2014), Effects of changing climate on the hydrology of a boreal catchment and lake DOC--Probabilistic assessment of a dynamic model chain, *Boreal Environ. Res.*, *19*, 66.

Hongve, D., G. Riise, and J. F. Kristiansen (2004), Increased colour and organic acid concentrations in Norwegian forest lakes and drinking water–A result of increased precipitation?, *Aquat. Sci.*, *66*(2), 231–238.

Ines, A. V., and J. W. Hansen (2006), Bias correction of daily GCM rainfall for crop simulation studies, *Agric. For. Meteorol.*, *138*(1), 44–53.

Intergovernmental Panel on Climate Change (2007), The physical science basis. Contribution of working group I to the fourth assessment report of the intergovernmental panel on climate change, in *Climate Change 2007: The Physical Science Basis*, edited by S. Solomon et al., 996 pp., Cambridge Univ. Press, Cambridge, U. K., and New York.

Jansson, P. E., M. Svensson, D. B. Kleja, and D. Gustafsson (2008), Simulated climate change impacts on fluxes of carbon in Norway spruce ecosystems along a climatic transect in Sweden, *Biogeochemistry*, *89*(1), 81–94, doi:10.1007/s10533-007-9147-6.

Karlson, K., R. Rosenberg, and E. Bonsdorff (2002), Temporal and spatial large-scale effects of eutrophication and oxygen deficiency on benthic fauna in Scandinavian and Baltic waters: A review, *Oceanogr. Mar. Biol.*, *40*, 427–489.

Kleja, D. B., et al. (2008), Pools and fluxes of carbon in three Norway spruce ecosystems along a climatic gradient in Sweden, *Biogeochemistry*, *89*(1), 7–25, doi:10.1007/s10533-007-9136-9.

Koehler, B., T. Landelius, G. A. Weyhenmeyer, N. Machida, and L. J. Tranvik (2014), Sunlight-induced carbon dioxide emissions from inland waters, *Global Biogeochem. Cycles*, *28*, 696–711, doi:10.1002/2014GB004850.

Kreutzweiser, D. P., P. W. Hazlett, and J. M. Gunn (2008), Logging impacts on the biogeochemistry of boreal forest soils and nutrient export to aquatic systems: A review, *Environ. Rev.*, *16*, 157–179.

Larsen, S., T. Andersen, and D. O. Hessen (2011), Climate change predicted to cause severe increase of organic carbon in lakes, *Global Change Biol.*, *17*(2), 1186–1192.

Laudon, H., J. Hedtjärn, J. Schelker, K. Bishop, R. Sørensen, and A. Ågren (2009), Response of dissolved organic carbon following forest harvesting in a boreal forest, *AMBIO: A J. Human Environ.*, *38*(7), 381–386.

Laudon, H., M. Berggren, A. Ågren, I. Buffam, K. Bishop, T. Grabs, M. Jansson, and S. Köhler (2011a), Patterns and dynamics of dissolved organic carbon (DOC) in boreal streams: The role of processes, connectivity, and scaling, *Ecosystems*, *14*(6), 880–893.

Laudon, H., R. A. Sponseller, R. W. Lucas, M. N. Futter, G. Egnell, K. Bishop, A. Ågren, E. Ring, and P. Högberg (2011b), Consequences of more intensive forestry for the sustainable management of forest soils and waters, *Forests*, *2*(1), 243–260.

Laudon, H., J. Buttle, S. K. Carey, J. McDonnell, K. McGuire, J. Seibert, J. Shanley, C. Soulsby, and D. Tetzlaff (2012), Cross-regional prediction of long-term trajectory of stream water DOC response to climate change, *Geophys. Res. Lett.*, *39*, L18404, doi:10.1029/2012GL053033.

Laudon, H., I. Taberman, A. Ågren, M. Futter, M. Ottosson-Löfvenius, and K. Bishop (2013a), The Krycklan Catchment Study—a flagship infrastructure for hydrology, biogeochemistry, and climate research in the boreal landscape, *Water Resour. Res.*, *49*, 7154–7158, doi:10.1002/wrcr.20520.

Laudon, H., D. Tetzlaff, C. Soulsby, S. Carey, J. Seibert, J. Buttle, J. Shanley, J. J. McDonnell, and K. McGuire (2013b), Change in winter climate will affect dissolved organic carbon and water fluxes in mid-to-high latitude catchments, *Hydrol. Processes*, *27*(5), 700–709, doi:10.1002/hyp.9686.

Leavesley, G. H. (1994), Modeling the effects of climate change on water resources-a review, *Clim. Change*, *28*(1–2), 159–177.

Ledesma, J., T. Grabs, M. Futter, K. H. Bishop, H. Laudon, and S. Köhler (2013), Riparian zone control on base cation concentration in boreal streams, *Biogeosciences*, *10*(6), 3849–3868.

Lepistö, A., M. N. Futter, and P. Kortelainen (2014), Almost 50 years of monitoring shows that climate, not forestry, controls long-term organic carbon fluxes in a large boreal watershed, *Global Change Biol.*, *20*(4), 1225–1237, doi:10.1111/gcb.12491.

Löfgren, S., E. Ring, C. von Brömssen, R. Sørensen, and L. Högbom (2009), Short-term effects of clear-cutting on the water chemistry of two boreal streams in northern Sweden: A paired catchment study, *AMBIO: A J. Human Environ.*, *38*(7), 347–356.

Magnani, F., M. Mencuccini, M. Borghetti, P. Berbigier, F. Berninger, S. Delzon, A. Grelle, P. Hari, P. G. Jarvis, and P. Kolari (2007), The human footprint in the carbon cycle of temperate and boreal forests, *Nature*, *447*(7146), 849–851.

Milestad, R., Å. Svenfelt, and K. H. Dreborg (2014), Developing integrated explorative and normative scenarios: The case of future land use in a climate-neutral Sweden, *Futures*, *60*, 59–71.

Muerth, M., B. Gauvin St-Denis, S. Ricard, J. Velázquez, J. Schmid, M. Minville, D. Caya, D. Chaumont, R. Ludwig, and R. Turcotte (2013), On the need for bias correction in regional climate scenarios to assess climate change impacts on river runoff, *Hydrol. Earth Syst. Sci.*, *17*(3), 1189–1204.

Müller, R. A., M. N. Futter, S. Sobek, J. Nisell, K. Bishop, and G. A. Weyhenmeyer (2013), Water renewal along the aquatic continuum offsets cumulative retention by lakes: Implications for the character of organic carbon in boreal lakes, *Aquat. Sci.*, *75*(4), 535–545.

Nabuurs, G.-J., M. Lindner, P. J. Verkerk, K. Gunia, P. Deda, R. Michalak, and G. Grassi (2013), First signs of carbon sink saturation in European forest biomass, *Nat. Clim. Change*, *3*, 792–796, doi:10.1038/NCLIMATE1853.

Naden, P. S., N. Allott, L. Arvola, M. Järvinen, E. Jennings, K. Moore, C. N. Aonghusa, D. Pierson, and E. Schneiderman (2010), Modelling the impacts of climate change on dissolved organic carbon, in *The Impact of Climate Change on European Lakes*, pp. 221–252, Springer, Netherlands.

Nash, J. E., and J. Sutcliffe (1970), River flow forecasting through conceptual models part I—A discussion of principles, *J. Hydrol.*, *10*(3), 282–290.

Oni, S., M. Futter, K. Bishop, S. Köhler, M. Ottosson-Löfvenius, and H. Laudon (2013), Long-term patterns in dissolved organic carbon, major elements and trace metals in boreal headwater catchments: Trends, mechanisms and heterogeneity, *Biogeosciences*, *10*(4), 2315–2330.

Oni, S., M. Futter, C. Teutschbein, and H. Laudon (2014), Cross-scale ensemble projections of dissolved organic carbon dynamics in boreal forest streams, *Clim. Dyn.*, *42*(9–10), 2305–2321, doi:10.1007/s00382-014-2124-6.

Öquist, M., K. Bishop, A. Grelle, L. Klemedtsson, S. Köhler, H. Laudon, A. Lindroth, M. Ottosson Löfvenius, M. B. Wallin, and M. B. Nilsson (2014), The full annual carbon balance of boreal forests is highly sensitive to precipitation, *Environ. Sci. Technol. Lett.*, *1*(7), 315–319.

Palviainen, M., L. Finér, A. Laurén, S. Launiainen, S. Piirainen, T. Mattsson, and M. Starr (2014), Nitrogen, phosphorus, carbon, and suspended solids loads from forest clear-cutting and site preparation: Long-term paired catchment studies from eastern Finland, *Ambio*, *43*(2), 218–233.

Pan, Y., R. A. Birdsey, J. Fang, R. Houghton, P. E. Kauppi, W. A. Kurz, O. L. Phillips, A. Shvidenko, S. L. Lewis, and J. G. Canadell (2011), A large and persistent carbon sink in the world's forests, *Science*, *333*(6045), 988–993.

Piani, C., J. Haerter, and E. Coppola (2010), Statistical bias correction for daily precipitation in regional climate models over Europe, *Theor. Appl. Climatol.*, *99*(1–2), 187–192.

Rankinen, K., T. Karvonen, and D. Butterfield (2004), A simple model for predicting soil temperature in snow-covered and seasonally frozen soil: model description and testing, *Hydrol. Earth Syst. Sci.*, *8*(4), 706–716.

Rounsevell, M. D., and M. J. Metzger (2010), Developing qualitative scenario storylines for environmental change assessment, *Wiley Interdiscip. Rev. Clim. Change*, *1*(4), 606–619.

Saikku, L., and E. Asmala (2010), Eutrophication in the Baltic Sea, *J. Ind. Ecol.*, *14*(3), 482–495.

Sanders, L., and M. W. McBroom (2013), Stream water quality and quantity effects from select timber harvesting of a streamside management zone, *South. J. Appl. For.*, *37*(1), 45–52.

Schelker, J., K. Eklöf, K. Bishop, and H. Laudon (2012), Effects of forestry operations on dissolved organic carbon concentrations and export in boreal first-order streams, *J. Geophys. Res.*, *117*, G01011, doi:10.1029/2011JG001827.

Schelker, J., T. Grabs, K. Bishop, and H. Laudon (2013a), Drivers of increased organic carbon concentrations in stream water following forest disturbance: Separating effects of changes in flow pathways and soil warming, *J. Geophys. Res. Biogeosci.*, *118*, 1814–1827, doi:10.1002/2013JG002309.

Schelker, J., L. Kuglerova, K. Eklöf, K. Bishop, and H. Laudon (2013b), Hydrological effects of clear-cutting in a boreal forest–Snowpack dynamics, snowmelt and streamflow responses, *J. Hydrol.*, *484*, 105–114.

Schelker, J., K. Öhman, S. Löfgren, and H. Laudon (2014), Scaling of increased dissolved organic carbon inputs by forest clear-cutting–What arrives downstream?, *J. Hydrol.*, *508*, 299–306.

Seibert, J., T. Grabs, S. Köhler, H. Laudon, M. Winterdahl, and K. Bishop (2009), Linking soil-and stream-water chemistry based on a Riparian Flow-Concentration Integration Model, *Hydrol. Earth Syst. Sci.*, *13*(12), 2287–2297.

Sørensen, R., M. Meili, L. Lambertsson, C. von Brömssen, and K. Bishop (2009a), The effects of forest harvest operations on mercury and methylmercury in two boreal streams: Relatively small changes in the first two years prior to site preparation, *AMBIO: A J. Human Environ.*, *38*(7), 364–372.

Sørensen, R., E. Ring, M. Meili, L. Högbom, J. Seibert, T. Grabs, H. Laudon, and K. Bishop (2009b), Forest harvest increases runoff most during low flows in two boreal streams, *AMBIO: A J. Human Environ.*, *38*(7), 357–363.

Stepanauskas, R. n., N. O. JØrgensen, O. R. Eigaard, A. Žvikas, L. J. Tranvik, and L. Leonardson (2002), Summer inputs of riverine nutrients to the Baltic Sea: bioavailability and eutrophication relevance, *Ecol. Monogr.*, *72*(4), 579–597.

Temnerud, J., J. K. Hytteborn, M. N. Futter, and S. J. Köhler (2014), Evaluating common drivers for color, iron and organic carbon in Swedish watercourses, *Ambio*, *43*(1), 30–44.

Tetzlaff, D., C. Soulsby, J. Buttle, R. Capell, S. Carey, H. Laudon, J. McDonnell, K. McGuire, S. Seibert, and J. Shanley (2013), Catchments on the cusp? Structural and functional change in northern ecohydrology, *Hydrol. Processes*, *27*(5), 766–774, doi:10.1002/hyp.9700.

Teutschbein, C., and J. Seibert (2012), Bias correction of regional climate model simulations for hydrological climate-change impact studies: Review and evaluation of different methods, *J. Hydrol.*, *456-457*, 12–29.

Teutschbein, C., and J. Seibert (2013), Is bias correction of regional climate model (RCM) simulations possible for non-stationary conditions?, *Hydrol. Earth Syst. Sci.*, *17*(12), 5061–5077.

Thorne, R. (2011), Uncertainty in the impacts of projected climate change on the hydrology of a subarctic environment: Liard River Basin, *Hydrol. Earth Syst. Sci.*, *15*(5), 1483–1492.

Tipping, E., C. Woof, E. Rigg, A. Harrison, P. Ineson, K. Taylor, D. Benham, J. Poskitt, A. Rowland, and R. Bol (1999), Climatic influences on the leaching of dissolved organic matter from upland UK moorland soils, investigated by a field manipulation experiment, *Environ. Int.*, *25*(1), 83–95.

Tiwari, T., H. Laudon, K. Beven, and A. M. Ågren (2014), Downstream changes in DOC: Inferring contributions in the face of model uncertainties, *Water Resour. Res.*, *50*, 514–525, doi:10.1002/2013WR014275.

Tranvik, L. J., J. A. Downing, J. B. Cotner, S. A. Loiselle, R. G. Striegl, T. J. Ballatore, P. Dillon, K. Finlay, K. Fortino, and L. B. Knoll (2009), Lakes and reservoirs as regulators of carbon cycling and climate, *Limnol. Oceanogr.*, *54*(6), 2298–2314.

Van der Linden, P., and J. F. B. Mitchell (2009), *ENSEMBLE: Climate Change and its Impacts: Summary of Research and Results From the ENSEMBLES Project*, Met Office Hadley Centre, FitzRoy Road, Exeter EX1 3PB, U. K.

van Vuuren, D. P., and T. R. Carter (2014), Climate and socio-economic scenarios for climate change research and assessment: Reconciling the new with the old, *Clim. Change*, *122*(3), 415–429.

Wallin, M. B., T. Grabs, I. Buffam, H. Laudon, A. Ågren, M. G. Öquist, and K. Bishop (2013), Evasion of CO2 from streams–The dominant component of the carbon export through the aquatic conduit in a boreal landscape, *Global Change Biol.*, *19*(3), 785–797.

Watts, G., R. W. Battarbee, J. P. Bloomfield, J. Crossman, A. Daccache, I. Durance, J. A. Elliott, G. Garner, J. Hannaford, and D. M. Hannah (2015), Climate change and water in the UK–past changes and future prospects, *Prog. Phys. Geogr.*, *39*(1), 6–28.

Wikner, J., and A. Andersson (2012), Increased freshwater discharge shifts the trophic balance in the coastal zone of the northern Baltic Sea, *Global Change Biol.*, *18*(8), 2509–2519.

Winterdahl, M., M. Futter, S. Köhler, H. Laudon, J. Seibert, and K. Bishop (2011), Riparian soil temperature modification of the relationship between flow and dissolved organic carbon concentration in a boreal stream, *Water Resour. Res.*, *47*, W08532, doi:10.1029/2010WR010235.

Winterdahl, M., M. Erlandsson, M. N. Futter, G. A. Weyhenmeyer, and K. Bishop (2014), Intra-annual variability of organic carbon concentrations in running waters: Drivers along a climatic gradient, *Global Biogeochem. Cycles*, *28*, 451–464, doi:10.1002/2013GB004770.

Woo, M.-K., R. Thorne, K. Szeto, and D. Yang (2008), Streamflow hydrology in the boreal region under the influences of climate and human interference, *Philos. Trans. R. Soc. B Biol. Sci.*, *363*(1501), 2249–2258.

Wu, H., C. Peng, T. Moore, D. Hua, C. Li, Q. Zhu, M. Peichl, M. Arain, and Z. Guo (2014), Modeling dissolved organic carbon in temperate forest soils: TRIPLEX-DOC model development and validation, *Geosci. Model Dev.*, *7*(3), 867–881.